Electrochemical Behaviors of Polyaniline–Poly(styrenesulfonic acid) Complexes and Related Films

Der-Shyu Lin, Cheng-Tung Chou, Yu-Wen Chen, Kung-Tu Kuo, Sze-Ming Yang

Department of Chemical and Materials Engineering, National Central University, Chung-Li, Taiwan 320, Republic of China

Received 22 December 2004; accepted 24 May 2005
DOI 10.1002/app.23231
Published online in Wiley InterScience (www.interscience.wiley.com).

ABSTRACT: This research focuses on the syntheses of polyaniline with poly(styrenesulfonic acid) and their electrochemical behavior, including absorbance behavior and electrochemical response time of polyaniline-poly(styrenesulfonic acid) [PANI–PSSA]. The complexes PANI–PSSA were prepared by electrochemical polymerization of monomer (aniline) with PSSA, using indium-tin oxide (ITO) as working electrode in 1*M* HCl solution. Polyaniline (PANI), poly(*o*-phenetidine)–poly(styrenesulfonic acid) [POP–PSSA], and poly(2-ethylaniline)–poly(styrenesulfonic acid) [P2E-PSSA] also were prepared by electrochemical polymerization and to be the reference samples. The products were characterized by IR, VIS, EPR, water solubility, elemental analysis, conductivity, SEM, and TEM. IR spectral studies shows that the structure of PANI–PSSA complexes is similar to that of polyaniline. EPR and visible spectra indicate the formation of polarons. The morphology of the blend were investigated by SEM and TEM, which indicate the conducting component and electrically conductive property of the polymer complexes. Elemental analysis results show that PANI–PSSA has a nitrogen to sulfur ratio (N/S) of 38%, lower than that for POP–PSSA (52%) and P2E–PSSA (41%). Conductivity of the complexes are around 10^{-2} S/cm, solubility of PANI–PSSA in water is 3.1 g/L. The UV-Vis. absorbance spectra of the hybrid organic/inorganic complementary electro-chromic device (ECD), comprising a polyaniline–poly(styrenesulfonic acid) [PANI–PSSA] complexes and tungsten oxide (WO_3) thin film coupled in combination with a polymer electrolyte poly(2-acrylamido-2-methyl-propane-sulfonic acid) [PAMPSA]. PANI–PSSA microstructure surface images have been studied by AFM. By applying a potential of ~3.0 V across the two external ITO contacts, we are able to modulate the light absorption also in the UV-Vis region (200–900 nm) wavelength region. For example, the absorption changes from 1.20 to 0.6 at 720 nm. The complexes PANI–PSSA, POP–PSSA, and P2E–PSSA were prepared by electrochemical polymerization of monomer (aniline, *o*-phenetidine, or 2-ethylaniline) with poly(styrenesulfonic acid), using ITO as working electrode in 1*M* HCl solution, respectively. UV-Vis spectra measurements shows the evidences for the dopped polyaniline system to be a highly electrochemical response time, recorded at the temperature 298 K, and the results were further analyzed on the basis of the color- discolor model, which is a typical of protontation systems. Under the reaction time (3 s) and monomer (aniline, *o*-phenetidine, 2-ethylaniline) concentration (0.6*M)* with PSSA (0.15*M)*, the best electrochemical color and discolor time of the PANI–PSSA is slower than POP–PSSA complexes (125/125 ms; thickness, 3.00 μm) and P2E–PSSA complexes. Under the same thickness (10 μm), the best electrochemical color and discolor time of the PANI–PSSA complexes is 1500/750 ms, that is much slower than P2E–PSSA complexes (750/500 ms) and POP–PSSA complexes (500/250 ms). In film growing rate, the PANI–PSSA complexes (0.54 μm/s) are slower than P2E–PSSA complexes (0.79 μm/s) and POP–PSSA complexes (1.00 μm/s), it can be attributed to the substituted polyaniline that presence of electro-donating (—OC_2H_5 or —$C_2H_{5)}$ group present in aniline monomer. The EPR spectra of the samples were recorded both at 298 K and 77 K, and were further analyzed on the basis of the polaron–bipolaron model. The narrower line-width of the substituted polyaniline complexes arises due to polarons; i.e., it is proposed that charge transport take place through both polarons and bipolarons, compared to their salts can be attributed to the lower degree of structural disorder, the oxygen absorption on the polymeric molecular complexes, and due to presence of electro-donating (—OC_2H_5 or —C_2H_5) group present in aniline monomer. J Appl Polym Sci 100: 4023–4044, 2006

Key words: conducting polymers; polyelectrolytes; water-soluble polymers; conjugated polymers

INTRODUCTION

Intrinsically conductive polymers (ICP) have been intensively studied since 1976; these studies focused on their potential technological applications, including electro-chromic devices,[1–4] batteries,[5–8] sensors, catalysis, capacitors, antistatic coatings, and gas separation membranes.[9–13] An electrochromic device is combined by optically transparent electrodes coated with complementary electrochromic materials and separated by an electrolyte, which may be either solid or liquid. All plastic and flexible electrochromic devices will facilitate new technological applications, such as in information display, storage, the automotive industry, and architecture. Several electrochromic materials have been studied for possible use in "smart window" ap-

Correspondence to: D.-S. Lin (77740271@alumni.tku.edu.tw).
Contract grant sponsor: The National Science Council of Republic of China.

plications[14,15,16] and color switching displays.[16,17] Smart windows may elegantly contribute to energy savings in buildings by dynamic control of the light absorbance and maximize the efficiency for heat and lighting control of office buildings. Dynamic control for heat flow and lighting through windows can reduce the air conditioning load for automobiles by an automatically controlled tint of sun roof.[18]

Conducting polymers are promising materials for electrochromic applications, which show attractive electric and optical properties, not only as colorants but also as conducting materials. Inorganic electrochromic materials can be combined with conducting polymers to extend the expected color change and reduce the operational potential. The use of conducting complexes are one way to improve electrochromic properties and are also useful in improving physical properties.[19] Polyaniline is a reversibly switchable material, the color changes from transparent to green, reversibly color-switched for 2.5×10^5 cycles,[18] and is easily deposited in thin films at ambient temperature on various substrates coated with indium-tin oxide (ITO).[20–23] Polyaniline with polyelectroylte[24] shows a high optical contrast between the reduced and the oxidized form. They are also more stable toward thermal treatment and have good adhesion; those characteristics make them suitable for use in electro-chromic displays.

Tungsten trioxide (WO_3) has been widely studied for the purpose of applying it to new passive display devices[25,26] (such as nonaqueous Li-salt solutions)[26] in the form of electrolyte and WO_3 films, as the electrochromic materials have been found to show a good response (0.5 s), a desirable coloration efficiency (50 C/m^2), and long life cycle ($>10^7$cycles).[27] Tungsten trioxide films have been prepared by various methods, including vacuum evaporation, supttering, coating, anodic oxidation, and electrode position.[28] Absorption spectra for polyaniline in the 300–1200 nm wavelength region are given by Ohsawa et al.[29] Transmission spectra for an electrochromic window based on tungsten oxide (WO_3) in the 350–2500 nm wavelength region have been studied by Stevens et al.[30] Including polyaniline and WO_3 coating, electro-chromic windows have been studied in the 350–800 nm wavelength region by Dao and Nguyen.[17] The classical tungsten oxide, as its oxides in bulk thin films are wavelength region by Dao and Nguyen.[17] The classical tungsten oxide as well as its oxides in bulk thin films is known to work quite well.

Polyaniline is unique among conducting polymers in that its electrical and structural properties can be reversibly controlled both by changing the oxidation state of the polymer main chain and protonation of the imine nitrogen atoms.[31,32] In this polymer, proton doping and dedoping is a reversible (switchable) process, the color change from transparent to green, reversibly color-switched for 2.5×10^5 cycles,[18] can easily be deposited on ITO. The adhesive properties and chemical inertness of poly(styrenesulfonic acid)[24] will make polyaniline blend suitable for conductive coating or electromagnetic interference (EMI) shielding, the substituted polyaniline salts have good electrochromic property,[33] with poly(styrenesulfonic acid) also can be used applied in electrochromic device,[24] hydrochloride acid presents very attractive properties as an electrochromic material with the good transport rate not only carried the positive charge as H^+ ion, lower molecular weight (MW = 1), fast delivery, lower formal potential but also its excellent and ideal electrolyte, is a good stronger electrolyte. The protonation-induced spin unpairing of polyaniline[34] causes a rearrangement of the structure, so, polyaniline is extremely paramagnetic.[35,36] To improve these characteristics polyaniline with poly(styrenesulfonic acid) was used as electrochromic material for the counter electrode. The stability of polyaniline with polyelectrolyte under air provides the opportunity of various applications, including improvement of the solubility of conducting polyaniline in water,[37] opens the opportunity for solution processing and blending, thus leading to materials with high electrical conductivity and mechanical strength.[38] Polyaniline[31,34,39–42] with polyelectrolyte[6] has material stability and dopants are part of the molecular complexes. It retains the good electro-optical properties of polyaniline, and is better than direct attachment of functional groups on instrinsically conductive polymers (ICP); the second strand provided functionality for solubility, blending compatibility, adhesion to devices, and resistance to heat and moisture.[43]

In this paper, we report the synthesis of polyaniline with polyelectrolyte, by the electrochemical polymerization of aniline with poly(styrenesulfonic acid) [PSSA] using ITO as working electrode, to study the UV-Vis absorption spectra of the electrochromic device in using indium-tin oxide (ITO) coated glass plates as transparent conductors and gluing the electrochromic coatings together with the solid polymer electrolyte PAMPSA, the two glass sandwiches become Glass/ITO/PANI-PSSA/PAMPSA/WO_3/ITO/Glass and Glass/ITO/PANI-PSSA/PAMPSA/ITO/Glass, respectively. An electrochromic window configuration based on the unsubstituted and substituted polyaniline with poly(styrenesulfonic acid) was measured, and their color and discolor time compared. UV-Vis absorption spectra of the electrochromic device in a window containing PANI–PSSA, POP–PSSA, or P2E-PSSA complexes, HCl and Pt, will be to investigated how much change in absorption modulation, electrochemical device become Glass/ITO/conducting polymer/HCl/Pt/Glass.

EXPERIMENTAL

Reagent

Reagent-grade aniline, re-distilled under nitrogen before use.

Films

For all device configurations unsubstituted polyaniline-poly(styrenesulfonic acid) complexes PANI–PSSA were electrochemically synthesized by cycling (50 mV/s), in the potential region −200 to +800 mV, ITO (1 mm × 50 mm × 10 mm) as the working electrode, Ag/AgCl as reference electrode, and platinum (Pt; 10 mm × 50 mm × 1 mm) as the auxiliary electrode; the reaction solution is 0.2*M* monomer (aniline) 7.5 mL with 0.2*M* poly(styrenesulfonic acid) 7.5 mL. The reference samples including poly(*o*-phenetidine)–poly(styrenesulfonicacid)[POP–PSSA], poly(2-ethylaniline)–poly(styrene sulfonic acid)[P2E-PSSA], and poly(*o*-ansidine)–poly(styrenesulfonic acid)[POA-PSSA] were also prepared, and optical characterization[6,43]was carried out *in situ* using a UV-Vis Spectrophotometer in the UV-Vis region.

The samples were also prepared by electrochemical polymerization of the substituted polyaniline salts including poly(*o*-phenetidine) [POP], poly(2-etylaniline) [P2E], and polyaniline [PANI], which were to be the reference samples.

WO_3 film

The electrolyte for the WO_3 formation was prepared by dissolving 2 g of tungsten in 10 mL 30% hydrogen peroxide and diluting with water to a total volume of 250 mL,[44] thus, giving a tungsten concentration of 0.003*M*. The tungsten oxide film was formed by a constant voltage of +700 mV for 300 s on ITO glass plates versus an Ag/AgCl reference electrode (3.5*M* KCl). Subsequently, the WO_3 films were heated at 140°C for 1 h.[44–46]

Polymer electrolyte

The solid polymer electrolyte poly(2-acrylamido-2-methyl propane sulfonic acid)[PAMPSA][46]was purchased (Aldrich Chemical Company Inc.).

Characterization

Spectral

FTIR spectra of the complexes were recorded on a Jasco 410 FT-IR spectrophotometer by the KBr pellet method; UV-Vis spectral data were obtained with a UV–Vis spectrophotometer (Jasco 7850); EPR Spectra were recorded at 298 K and 77 K, in air and argon, using a EMX-10 (Bruker) EPR spectrometer operating in the X band and equipped with a liquid nitrogen cooled temperature controller.

Solubility

Solubility measurements were carried out by dissolving the substituted polyaniline complexes [PANI–PSSA, P2E–PSSA, or POP–PSSA] in water, suction-filtering the solution through a 0.2-μm filter membrane, extracting 100 mL of the solutions with a syringe, and drying at 60°C to a constant weight.

Elemental analysis

Elemental analysis was done using a Heraeus CHNOS Rapid F002 Elemental Analyzer (Gemmary) on 5-to 10 mg samples.

Conductivity measurement

The four-probe method was used for the measurement of the conductivity of the sample films; a Keithley Model 238 programmable current source and voltmeter error was less than 2%.

AFM measurement

The polymer blend of the PANI–PSSA complexes films on the ITO was obtained by the electrochemical syntheses method, then by cleaning with 2 mL 1*M* HCl (aq), and drying through 65°C for 2 h. AFM images were obtained on a Digital Instrument DI 5000 in the National Nano Device Lab.

Morphology measurement

Transmission electron imaging (TEM) were performed on a JEM-2000 FXII microscope, operated at 160 kV. Scanning electron micrograph (SEM) was performed on a Hitachi S-3500 microscope, to study the morphology of the conductive fibers at an accelerating voltage of 20 kV, and the samples were gold-sputtered before observation.

Device configuration

An all plastic and flexible solid-state electrochromic device using PANI–PSSA complexes and WO_3 deposited on ITO and a polymeric electrolyte (PAMPSA).

The device was constructed under atomspheric conditions and showed good optical characterisitics. A cross-sectional view, which uses electrodeposition amorphous tungsten trioxide (WO_3) films as the electrochromic material, a polymer proton conductors (PAMPSA) as the electrolyte, and a PANI-PSSA on ITO electrode as the working electrode and Pt elec-

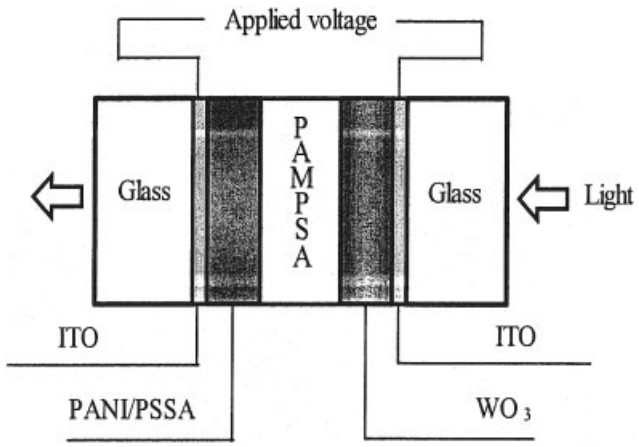

Figure 1 A schematic drawing of the electrochromic devices glass/ITO/WO_3/PAMPSA/PANI–PSSA/ITO/glass system showing the different materials and layers used.

trode as the counter electrode, is shown in Figure 1. A substrate glass of the display electrode was coated with an ITO thin film to diminish proton and electron migration, which give rise to cell degradation,[47] from the substrate glass into WO_3 film through ITO, the complexes of PANI–PSSA were formed on ITO by an electrochemical method. The electrochromic windows were fabricated by adding the electrolyte solution onto the PANI–PSSA and WO_3 substrates film, heating at 70°C for 5 min, and joining them together while the PAMPSA was still sticky. During 24 h at room temperature, the electrolyte hardens and binds the two substrates together. The electrochromic device is shown in Figure 1, with dimensions 1 cm × 4.5 cm × 0.8 cm, the PAMPSA layer thickness is in the order of 1 mm, and the PANI–PSSA and WO_3 layers are thinner than 30 μm. The electrochemical deposition of PANI–PSSA and WO_3 and the potential cycling were performed using a computer controlled BAS-100B electrochemical analysis. A UV-Vis spectrophotometer (Jasco 7850) was used to measure the absorbance in the ultraviolet and visible region. The absorbance spectra were recorded under potentiostatic control, and to stabilize the electrochromic PANI–PSSA and WO_3 films, the window was held at a constant potential for 5 min before recording the absorbance spectra.

Absorbance measurement

The electrochromic devices cell ITO/PANI–PSSA, POP–PSSA or P2E–PSSA/HCl/Pt system showing the different materials and layers used. The unsubstituted polyaniline complexes, PANI–PSSA, is to be measured and compare their color and discolor time, the reference samples including polyaniline (PANI), poly(2-ethylaniline) [P2E], poly(*o*-phenetidine) [POP], POP–PSSA, and P2E–PSSA complexes were electrochemical polymerization,[45] the absorption spectra of the films deposited on glasses were recorded with a UV/VIS spectrometer(Jasco Model 7850), by using an uncoated glass as a reference electrode (shown in Fig. 2). At a fixed wavelength of 630 nm, the relation between the film thickness determined by the reaction time and monomer concentration with a Electrochemical Analyzer (BAS 100). Film thickness, calculated from the nano-spectrometer, is the average of five times of measurement. Both safe voltage operation and the color are reversible to measurement of the color and discolor time.

Calculate color and discolor time

Electrochemical response time calculated from the absorption that during color and discolor for substituted polyaniline complexes, color time ($t_{c;}t_{\text{color}}$) is calculated from color the absorption arrived 50%; Discolor time ($t_{d;}\, t_{\text{discolor}}$) is calculated from discolor the absorption arrived 50%,and is shown as the Figure 3. The color changes of polyaniline, poly(*o*-phenetidine), and poly(2-ethylaniline) with/without PSSA by electrochromic device in 1*M* HCl electrolyte were cycled at a 50 mV/s sweep rate, cycling between −200 and 800 mV/SCE was performed.

EPR spectra

The EPR spectra were obtained for the powder samples at different temperatures both 298 K and 77 K in the air and argon using a EMX-10 (Bruker) spectrometer operating in the X band and equipped with a liquid nitrogen-cooled temperature controller.

RESULTS AND DISCUSSION

Synthesis

The electrochemical polymerization of the substituted polyaniline with poly(styrenesulfonic acid) complexes PANI–PSSA, POP–PSSA, and P2E–PSSA and their conductivity are presented in Table I.

Characterization

IR spectra

The infrared spectra of the polyaniline–polyelectrolyte complexes PANI–PSSA, POP–PSSA, P2E–PSSA and their salts are shown in Figures 4 and 5, that prepared from monomer [aniline, *o*-phenetidine, and 2-ethylaniline] with poly(styrenesulfonic acid) in 1*M* HCl, respectively, are very nearly the same, which in turn closely matches the infrared spectrum of the polyaniline base prepared form polyaniline hydrochloride. The IR absorption bands are at ~1600 cm^{-1} (C═C stretching in quionoid unit), ~1500 cm^{-1}(C═C

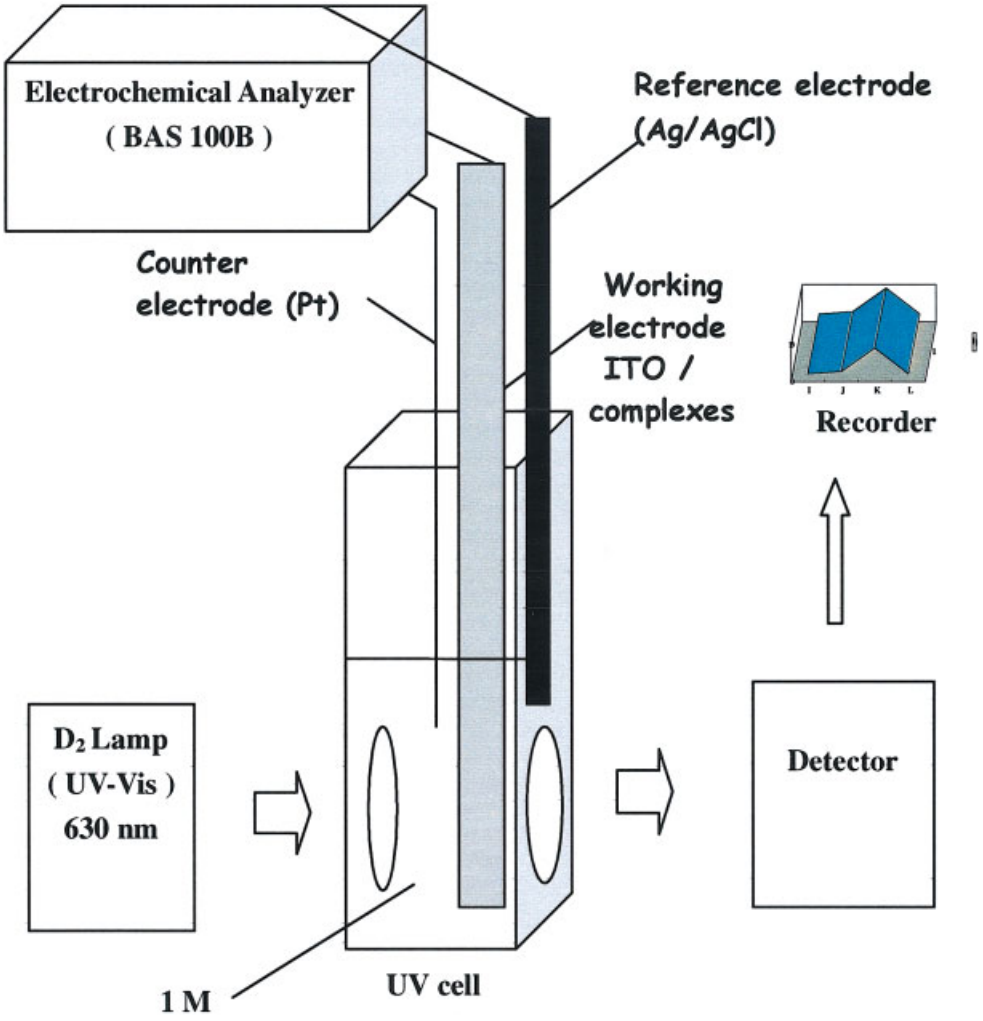

Figure 2 Electrochemical response time measured apparatus. [Color figure can be viewed in the online issue, which is available at www.interscience.wiley.com.]

stretching in benzonoid unit) ,1200, 1040, and 1020 cm^{-1} (—SO_3H), 1100 cm^{-1}(aromatic C—O stretching), 930–800 cm^{-1} and 770–750 cm^{-1} (1,2,4-trisubstituted phenyl ring).

UV-Vis spectra

The UV-Vis absorption peaks of PANI–PSSA, POP–PSSA, and P2E–PSSA, in water are presented in Table II and Figure 6. The products showed absorption peaks at ~420 and ~800 nm in the visible region; and an absorption peak at 550–630 nm appeared, the spectral changes indicate the formation of the base form. However, the absorption peak of PANI–PSSA, POP–PSSA, and P2E–PSSA shifts to near ~580 nm, indicating a higher oxidation state than in emeraldine salts. Solutions of PANI–PSSA, POP–PSSA, and P2E–PSSA complexes can be chemically doped by acid (1*M* HCl) and undoped by base [0.1*M* NH_3 (aq)] to go through the normal sequence of reversible color changes from

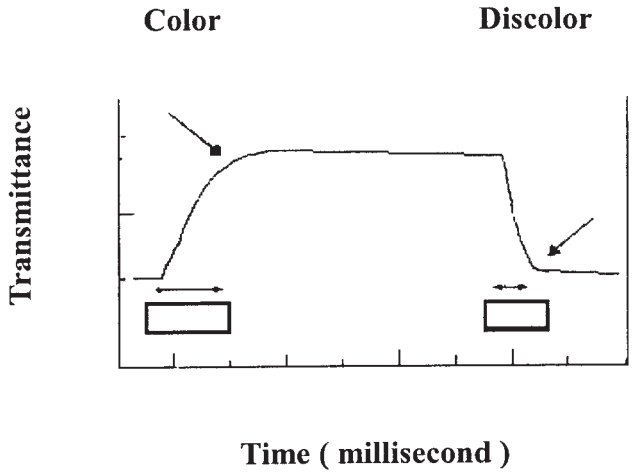

Figure 3 The electrochemical response time calculated form the absorption that during the color and discolor for substituted polyaniline complexes[color time (t_c) is t_{color}; discolor time (t_d) is $t_{discolor}$, show as the figure].

TABLE I
Conductivity of the Substituted Polyaniline Complexes

Sample	Conductivity ($\times 10^{-2}$ S/cm)
PANI–PSSA	4.7
POP–PSSA	3.8
P2E–PSSA	2.4

transparent green to blue. The spectra of PANI–PSSA, POP–PSSA, and P2E–PSSA complexes in aqueous solution have shown that the doped and undoped forms have the same spectra as that of the ordinary PANI[48]; this indicates that the POP–PSSA and P2E–PSSA complexes have the same electronic structures as the PANI–PSSA complexes.[49]

Deprotonation

The UV-Vis absorption spectra were recorded as the titration of PANI–PSSA, POP–PSSA, and P2E–PSSA with 0.1*M* NH_3 (aq) progressed; the clear, dark-green solution can change color according to the acid–base reactions, the λ_{max} were ~550 and ~800 nm for PANI–PSSA, ~580 and ~820 nm for P2E–PSSA, ~780 and ~620 nm for POP–PSSA; and pH value for each spectrum, at the corresponding pH and wavelength. The absorbance changed very little during the initial stage of titration when free HCl or excess sulfonic acid group in the solution were being neturalized; as more base was added, the color changed to blue, at pH 10.0 for PANI–PSSA,[45,46,50] at pH ~8.0 for POP–PSSA (Fig. 7), and at ~9.5 for P2E–PSSA (Fig. 8). The initial deprotonation were monitored at a wavelength of 550 nm for PANI–PSSA; 580 nm for P2E–PSSA; 620 nm for POP–PSSA; the pH value for deprotonation is higher than that of the HCl salts of substituted polyaniline,

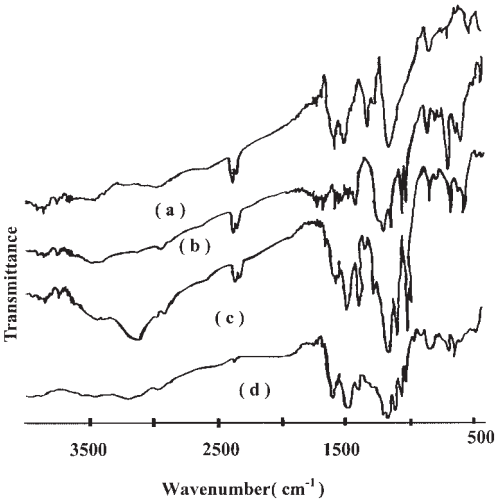

Figure 4 IR spectra of polyaniline complexes (a) PANI, (b) PANI-PSSA, (c) POP–PSSA, and (d) P2E–PSSA.

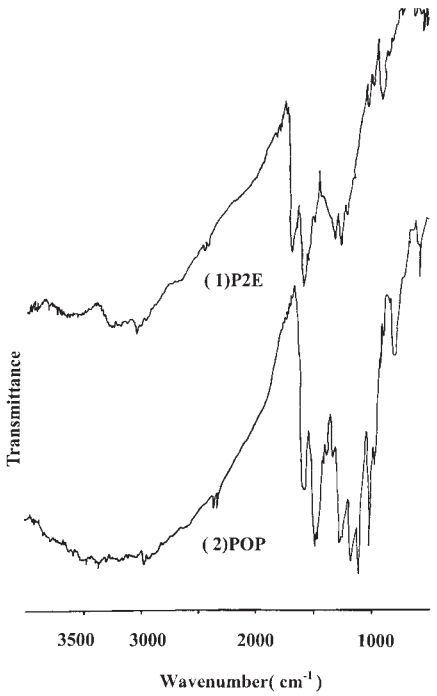

Figure 5 IR spectra of polyaniline salts (1) P2E and (2) POP.

the results indicate intimate interactions between two polymer chains. As more reductant were added to the solution, the absorbance at ~550 nm for PANI–PSSA, ~620 nm for POP–PSSA, ~580 nm for P2E–PSSA increased, and the ~800 nm band leveled off, which indicated that the complexes were close to their fully reduced leuco forms.

The stability of the PANI–PSSA, POP–PSSA, and P2E–PSSA complexes seems to be established by the attractive forces between the secondary amine of substituted polyaniline and the sulfonic acid group of poly(styrenesulfonic acid) within the complexes; the complexes PANI–PSSA, POP–PSSA, and P2E–PSSA are soluble in water and are easily dispersed into various coating systems. Direct interaction with oxiding agents (1*M* HCl) should be avoided to minimize loss in conductivity of the PANI–PSSA, POP–PSSA, and P2E–PSSA complexes, deprotonation of the polyaniline could occur with an organic base such as amine (0.1*M* NH_3, aqueous).

TABLE II
The max. UV-Vis Absorption Peaks of the Substituted Polyaniline Complexes

	λ_{max} (nm)	
Sample	Acid form	Base form
PANI–PSSA	800,420	550
P2E–PSSA	820,420	580
POP–PSSA	780,440	620

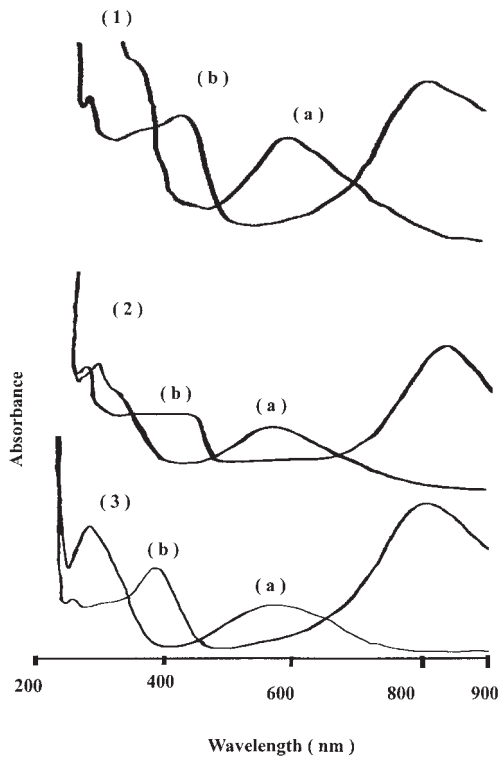

Figure 6 UV-Vis spectra of polyaniline complexes (1) PANI–PSSA; (2) POP–PSSA, and (3) P2E–PSSA; (a) acid form and (b) base form.

The PANI–PSSA, POP–PSSA, and P2E–PSSA complexes do not get easily dedoped by either heating[51] or water extraction. A unique feature of polyanilines in the emeraldine oxidation state is that they can be reversibly converted between conductive and insulating forms by an acid/base reaction; emeraldine base is

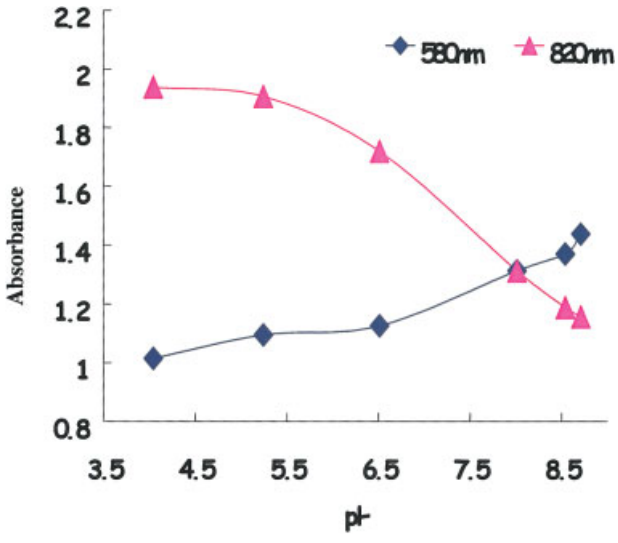

Figure 7 Deprotonation of POP–PSSA complexes by adding 0.1*M* NH_3 (aq). [Color figure can be viewed in the online issue, which is available at www.interscience.wiley.com.]

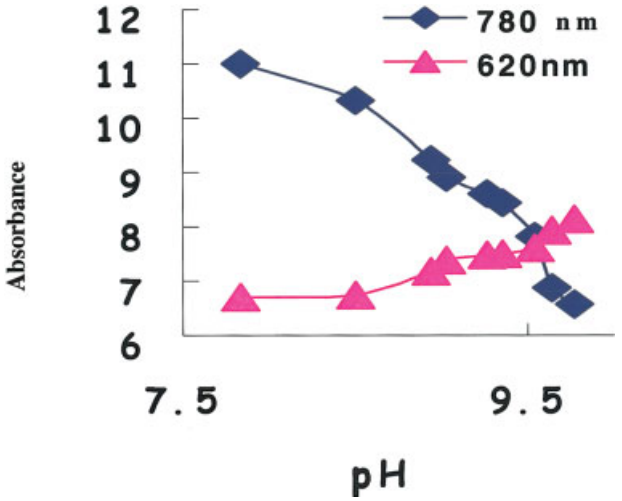

Figure 8 Deprotonation of P2E–PSSA complexes by adding 0.1*M* NH_3 (aq). [Color figure can be viewed in the online issue, which is available at www.interscience.wiley.com.]

a weak organic base ($pk_a \sim 5$), which when treated with an acid (1*M* HCl) of lower pk_a will react to become the conductive salt form; in the reverse procedure, the conductive form can be converted back to the insulating form by exposure to an organic base [0.1*M* NH_3 (aq)].

Elemental analysis

The results of elemental analysis and solubility studies on the unsubstituted and substituted polyaniline complexes are shown in the Tables III and IV, respectively. The elemental analysis indicates that the products have specific chemical compositions and are consistent with the formation of PANI–PSSA, P2E–PSSA, and POP–PSSA molecular complexes; the effect of sulfonic acid group on the polyaniline backbone, aimed at delineating the significant changes in polyaniline upon going from external protonic doping to internal doping, shows the formation of self-doped conducting polymers PANI–PSSA, POP–PSSA, and P2E–PSSA complexes; those polymer complexes have a wide range of solubility, which improves the processibility of the polymer. Elemental analysis (Table III) show that the values of N/S for the complexes are 38% for PANI–PSSA, 41% for P2E–PSSA, and 52% for POP–PSSA. Comparative studies of polyaniline salt and its polyelectrolyte complexes show similarities because of the same backbone structure and differences of the —SO_3H group on the polyelectrolyte template, the role of the —SO_3H (and —SO_3—) groups play in affecting the solubility, doping mechanism, and charge transport in the polyaniline system. The N/S ratio of the PANI–PSSA complexes is nearly 38% and is a double strand complex, which means it is a double strain structure. The main chains is emeraldine

TABLE III
Elemental Analysis of the Substituted Polyaniline Salts and Complexes

Sample	Relative ratios C	H	N	S	Experimental	Theoretical
POP	1	1.13	0.12	0	$C_{32}H_{36.7}N_{3.8}O_{8.2}$	$C_{32}H_{40}N_4O_4$
P2E	1	1.06	0.13	0	$C_{32}H_{33.4}N_{3.2}$	$C_{32}H_{40}N_4$
PANI	1	1.08	0.16	0	$C_{24}H_{26}N_{3.7}$	$C_{24}H_{20}N_4$
	N	S	C	H		
POP–PSSA	1	1.93	29.18	45.24	$N_{36}S_{69}C_{1051}H_{1629}O_{641.7}$	$N_{36}S_{69}C_{843}H_{776}O_{244}$
P2E–PSSA	1	2.43	21.55	31.3	$N_{24}S_{58}C_{517}H_{752}O_{246.5}$	$N_{24}S_{58}C_{658}H_{590}O_{175}$
PANI–PSSA	1	2.65	35.96	50.68	$N_{16}S_{42}C_{575}H_{811}O_{63}$	$N_{16}S_{42}C_{435}H_{335}O_{127}$

salts (i.e., N), which interact with the poly(styrenesulfonic acid) (i.e., S) chain by lone-pair induced interaction, while the other 1.65 poly(styrenesulfonic acid) chain containing sulfonic acid (—SO_3H) functional groups is left free, with no interaction with emeraldine salts. The latter free groups can increase the solubility in water (3.1 g/L). The N/S ratio of the P2E–PSSA complexes is nearly 41% and is a double strand complex, which means it is a double strain structure. The main chains is emeraldine salts (i.e., N) which interact with the poly(styrenesulfonic acid) (i.e., S) chain by lone-pair induced interaction, while the other 1.43 poly(styrenesulfonic acid) chain containing sulfonic acid (—SO_3H) functional groups is left free, with no interaction with emeraldine salts. The latter free groups can increase the solubility in water (2.9 g/L). The N/S ratio of the POP–PSSA complexes is nearly 52% (lager than that of the PANI–PSSA complexes); it is also a double-strand complexes, which means emeraldine salts have one lone-pair induced interaction with the poly(styrenesulfonic acid) chain, and have the other 0.93 poly(styrenesulfonic acid) chain containing sulfonic acid (—SO_3H) functional groups left free, increasing the solubility in water (1.9 g/L).

Solubility

The solubility results of PANI–PSSA, P2E–PSSA, and POP–PSSA complexes in water are shown in Table IV. The solubility is 3.1 g/L for PANI–PSSA, 2.9 g/L for P2E–PSSA, and 1.9 g/L for POP–PSSA. The complexes PANI–PSSA, POP–PSSA, and P2E–PSSA are not soluble in tetrahydrofuran, acetonitrile, 2-isopropanol, and methanol (Table V),but is a water soluble polymer.

TABLE IV
Elemental Analyses (N : S Ratio) of the Substituted Polyaniline Complexes and Solubility (in D.I water)

Sample	N : S	N/S (%)	Solubility (g/L)
POP–PSSA	1 : 1.93	52	1.9000
P2E–PSSA	1 : 2.43	41	2.9000
PANI–PSSA	1 : 2.65	38	3.1000

EPR spectra

EPR spectra of substituted polyaniline-HCl salts and their complexes show a single Lorentzian shaped signal (Fig. 9)without any hyperfine spitting in air and argon (Tables VI and VII). The g values of all the substituted polyaniline hydrochloride salts and their complexes lie around 2.00290–2.00321, which is almost the free electron g value, and suggests that polyaniline exists primarily as the polysemiquinone radical cation. The g value and line-width are found to be temperature-dependent; this g value, typical of π radicals in conjugated carbon systems, is consistent with the unpaired delocalized spin, primarily on the phenyl ring.

EPR is a powerful tool for probing spin localization and dimensionality through the measurement of spin concentration, g value, line-width, and line shape. The EPR line-width is determined by the relaxation time (T_2). Several relaxation processes can cause the shortening of T_2, and hence, the broadening of an EPR line, one of them being the spin-lattice relaxation characterized by a time constant (T_1).[52,53] The narrower line-width in polyaniline complexes [PANI–PSSA, POP–PSSA, and P2E–PSSA] compared with that of their salts [PANI, POP, and P2E] can be attributed to the lower degree of structural disorder, and the oxygen

TABLE V
The Sample of PANI–SSA, POP–PSSA, and P2E–PSSA Complexes are Insoluble in Organic Solvent Used

Solvent	PANI–PSSA	P2E–PSSA	POP–PSSA
Tetrahydrofuran	—[a]	—	—
Acetonitrile	—	—	—
Isopropanol	—	—	—
Methanol	—	—	—

[a] Precipitates are not soluble in organic solvent used

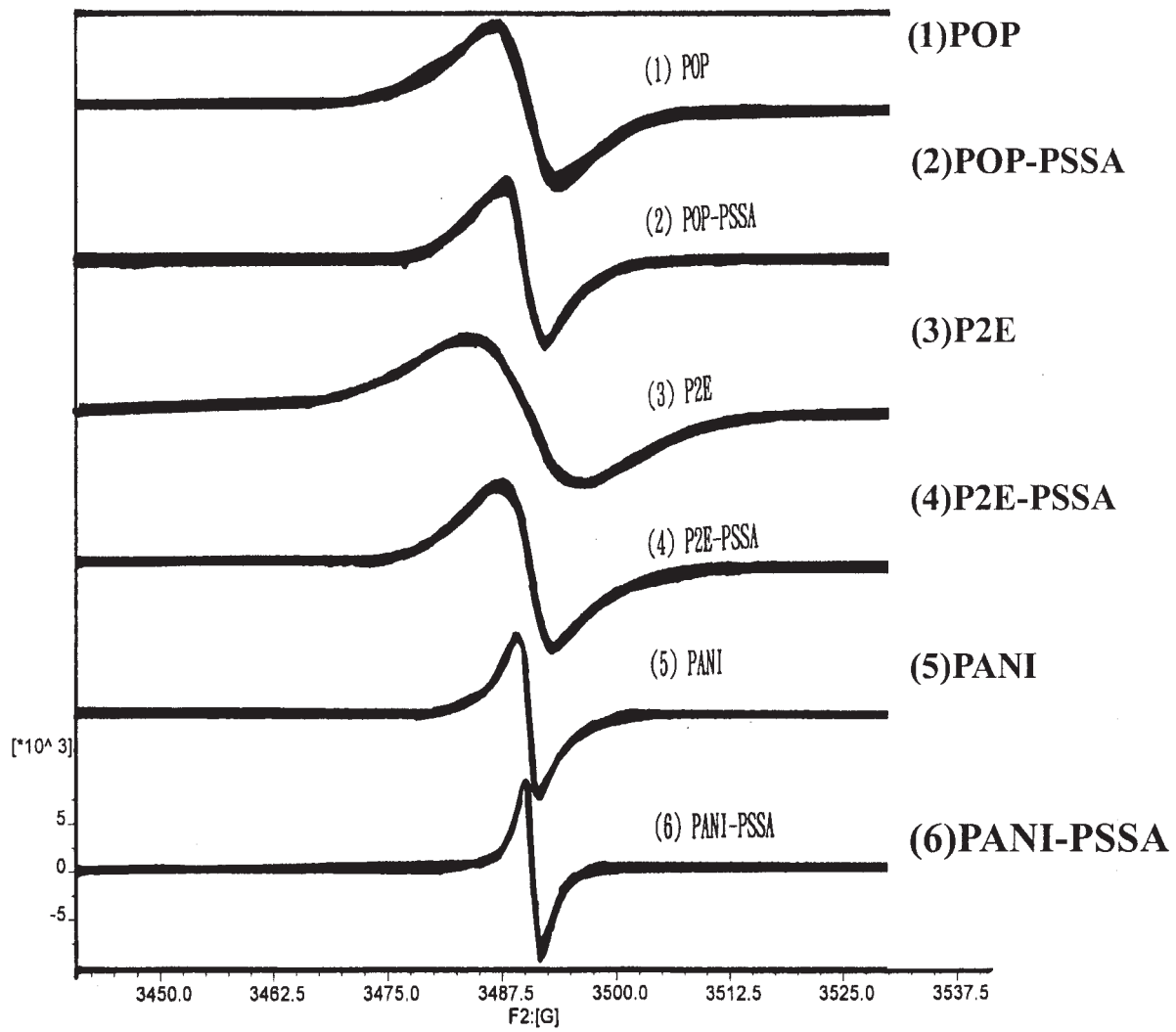

Figure 9 EPR spectra polyaniline complexes of (1) POP, (2) POP–PSSA, (3) P2E, (4) P2E–PSSA, (5) PANI and (6) PANI–PSSA.

absorption on the polymer molecular complexes.[54,55] The substituted polyaniline have side chain effect by the alkyl group (—C_2H_5 or —OC_2H_5) and the —SO_3H group on the polyelectrolyte template, with higher density[56] in their molecules complexes to form a different crystal structure. The EPR spectra also give evidence for the existence of highly mobile radical cations or polarons in PANI–PSSA, POP–PSSA, and P2E–PSSA complexes. Temperature-dependent transport property suggests that all polyaniline complexes show a single fine signal, without any hyperfine splitting structure.

TABLE VI
EPR Results of Substituted Polyaniline Complexes Under Air

	298 K		77 K	
Sample	Δ*H*pp (G)	*g* value	Δ*H*pp (G)	*g* value
POP	7.161	2.00304	9.577	2.00317
POP–PSSA	5.258	2.00302	6.177	2.00315
P2E	12.227	2.00319	14.089	2.00312
P2E–PSSA	6.091	2.00298	8.469	2.00292
PANI	2.270	2.00299	1.942	2.00298
PANI–PSSA	1.626	2.00296	1.537	2.00300

TABLE VII
EPR Results of Substituted Polyaniline Complexes Under Argon

	298 K		77 K	
Sample	Δ*H*pp (G)	*g*-value	Δ*H*pp (G)	*g*-value
POP	4.665	2.00300	5.835	2.00305
POP–PSSA	4.454	2.00301	5.909	2.00321
P2E	7.183	2.00300	10.344	2.00298
P2E–PSSA	5.448	2.00298	7.830	2.00299
PANI	0.965	2.00300	1.437	2.00294
PANI–PSSA	1.356	2.00290	1.483	2.00294

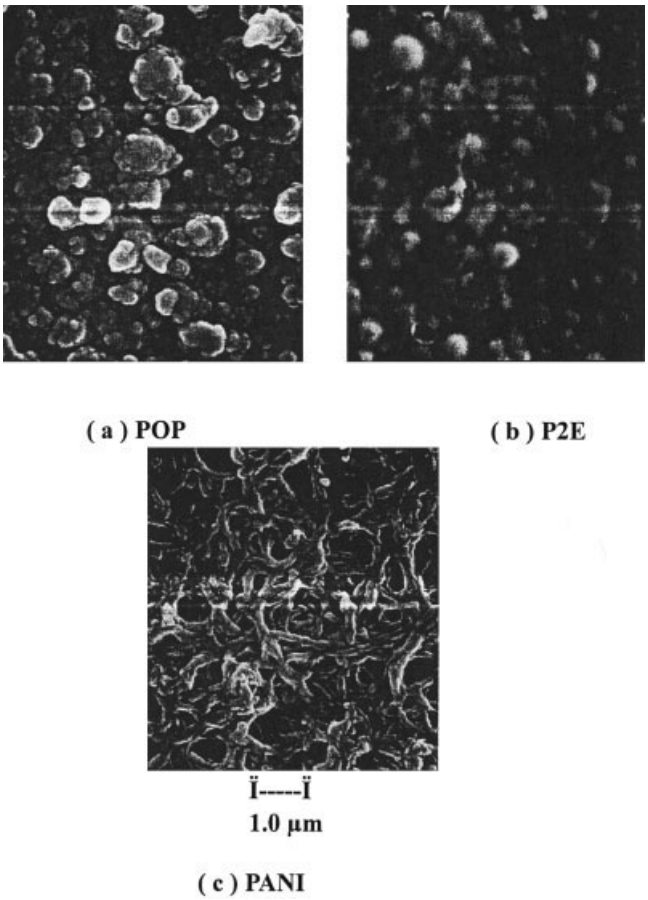

Figure 10 SEM micrographs of polyaniline complexes (a) poly(*o*-phenetidine)[POP], (b) poly(2-ethylaniline[P2E], and (c) polyaniline[PANI] (20 kV; ×30,000).

Conductivity

The conductivity of the complexes PANI–PSSA (4.7 × 10^{-2} S/cm), P2E–PSSA (2.4 × 10^{-2} S/cm), and POP–PSSA(3.8 × 10^{-2} S/cm) were ~10^{-2} S/cm (Table I); as well as the EPR data give evidence for the existence of highly mobile radical cations or polarons in the substituted polyaniline salts and their complexes, to be localizated since the samples are heavily doped and lower disordered.

Morphology

The SEM micrographs of polyaniline, poly(*o*-phenetidine), and poly(2-ethylaniline) (Fig. 10) show that the surface morphology of polyaniline is a network structure, poly(*o*-phenetidine) is the particulate structure, and poly(2-ethylaniline) is globular in structure. The micrographs of POP–PSSA, P2E–PSSA, and PANI–PSSA (Fig. 11) show that the surface morphology of PANI–PSSA is globular with irregular structure, POP–PSSA is a film with porous structure, and P2E–PSSA is globular and has irregular structure.

The TEM micrographs of PANI–PSSA complexes shown in Figure 12 ((a) 120,000×; (b) 150,000×; (c) 100,000×) correspond to different magnifications. As shown in figures, the polyaniline particulates should have distributed in the poly(styrenesulfonic acid) polyelectrolyte (Fig. 12(a)), would have been circular (Fig. 12(b)), and particulates connected together (Fig. 12(c)), and to form a channel useful the electron transfer. The TEM micrographs of P2E–PSSA complexes shown in Figure 13 ((a) 120,000×; (b) 150,000×; (c) 200,000×; (d) 100,000×) corresponds to different magnifications; as shown in figures, the poly(2-ethylaniline) particulates would have been circular (Fig. 13(a)) and should have been distributed in the poly(styrenesulfonic acid) polyelectrolyte (Fig. 13(b)) particulates connected together (Fig. 13(c)) to form a channel (Fig. 13(d)) useful for the electron transfer. Figure 14(a)–14(d) shows the TEM micrographs of the POP–PSSA complexes, with different magnifications ((a) 120,000×; (b) 150,000×; (c) 200,000×; (d) 100,000×); it can seen that the shape of the poly(*o*-phenetidine) is

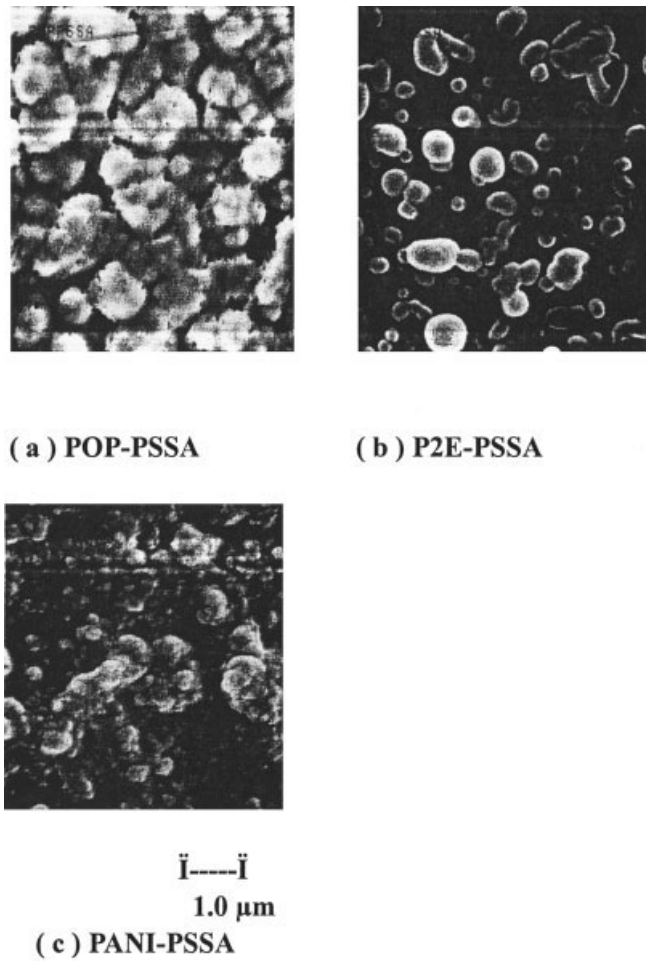

Figure 11 SEM micrographs of polyaniline complexes (a) POP–PSSA, (b) P2E–PSSA, and (c) PANI–PSSA (20 kV; ×30,000).

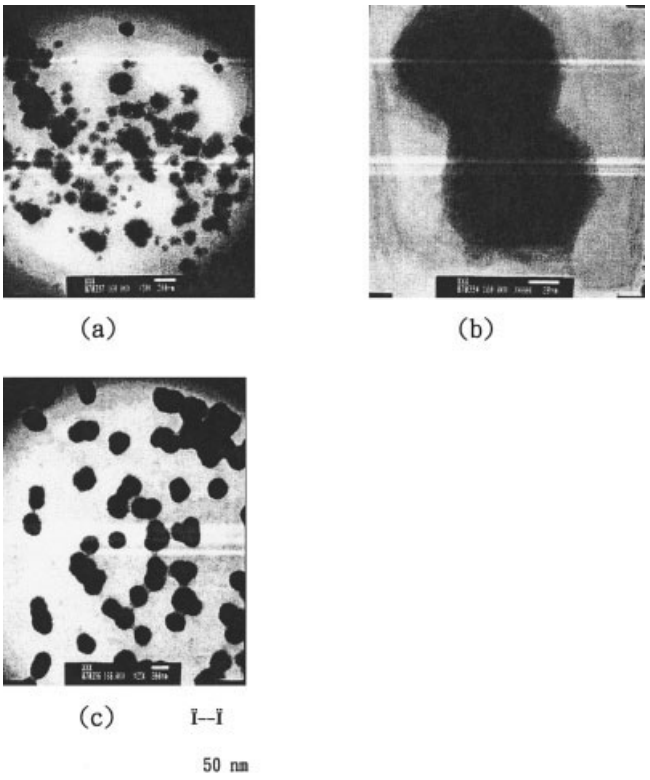

Figure 12 TEM micrographs of PANI–PSSA complexes [160 kV; (a) ×120,000; (b) ×150,000; (c) ×100,000].

particulates type morphology, this indicates (Fig. 14(d)) the intramolecular interaction between poly(*o*-phenetidine) and poly(styrenesulfonic acid) crosslink[57] introduced into the POP–PSSA complexes; the crosslink characteristics of each poly(*o*-phenetidine) were connected by particulates arrangement. The POP–PSSA complexes, measured by TEM, were shown as the particulates of poly(*o*-phenetidine) in complexes reacted with poly(styrenesulfonic acid) polyelectrolyte crosslink, subsequent to form a channel, useful for the electron transfer.

Cyclic voltammograms (50 mV/s) of the polyaniline (PANI) film and PANI–PSSA film on ITO, in the potential region −200 to +700 mV, are shown in Figures 15 and 16. Two oxidation state peak show polyaniline peak characters are 0.5 and −0.1 V, respectively. By applying a positive potential to the PANI and PANI–PSSA film, both PANI and PANI–PSSA obtain a blue color, while the PANI and PANI–PSSA film are discolored (both PANI and PANI–PSSA are −200 mV) by reverse cycles.[44] The AFM topography of PANI–PSSA blend on ITO without and with phase detector are shown in Figure 17. Polymer blends of PANI–PSSA complexes were studied in nanometer scale, the images of AFM show the topography of the blends. The results of AFM using phase detector show that the phase rich in poly(styrenesulfonic acid) are in the center of the particulate and the phase rich in polyaniline salt are around the particulate. A combination of AFM provides a good way to study the distribution of conductive polyaniline in the blend. The dark area of the AFM image with phase detector indicates the area of phase retardation. When AFM probe tapping was carried out on sticky material, large phase retardation were observed. In a comparison of the images with and without phase detector, it was found that the dark area was located in the center of the particle and the light area was located around the particulate. The results indicate that the center part of the particulate are rich in poly(styrenesulfonic acid) and the area around the particulate are rich in polyaniline complexes. The X-ray diffraction of WO_3 compound results are shown in Figure 18 that electrodeposited films were amorphous[58,59] when they were heat-treated for 1 h at temperatures below 300°C (i.e., 140°C). The results [$2\Theta = 24°$ for (010); 27° for (10 1 6)] indicate that electrodeposited films consisted of very small microcrystal.[60] The infrared spectra for electrodeposited films on ITO films formed on glass substrates are shown in Figure 19. Here, the spectra were measured by IR apparatus (Jasco; FT-IR 410), as can be seen from Figure 19, very strong and broad absorption peaks (~1600 and ~3500 cm^{-1}) of water were observed for the deposited films. However, the spectrum for the electro-deposited film after treatment shows

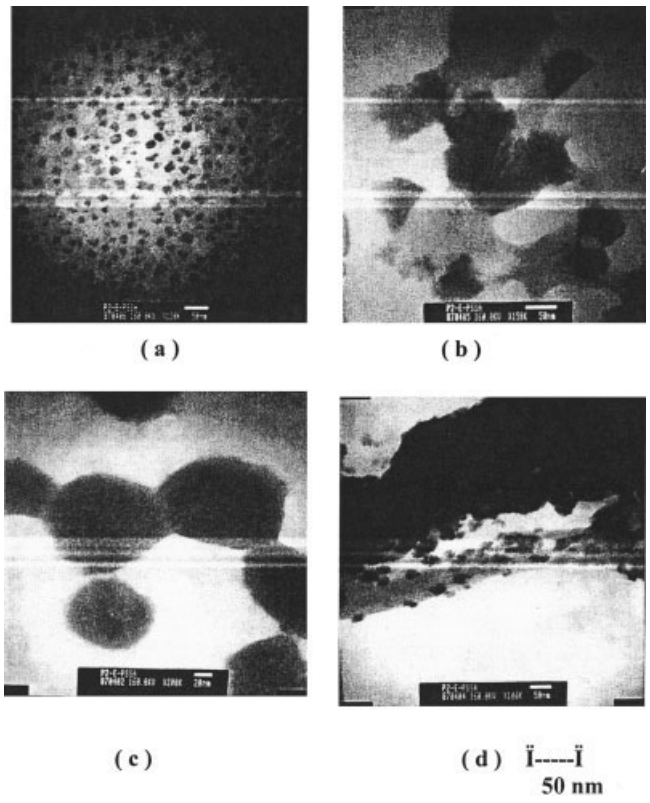

Figure 13 TEM micrographs of P2E–PSSA complexes [160 kV; (a) ×120,000; (b) ×150,000; (c) ×200,000; (d) ×100,000].

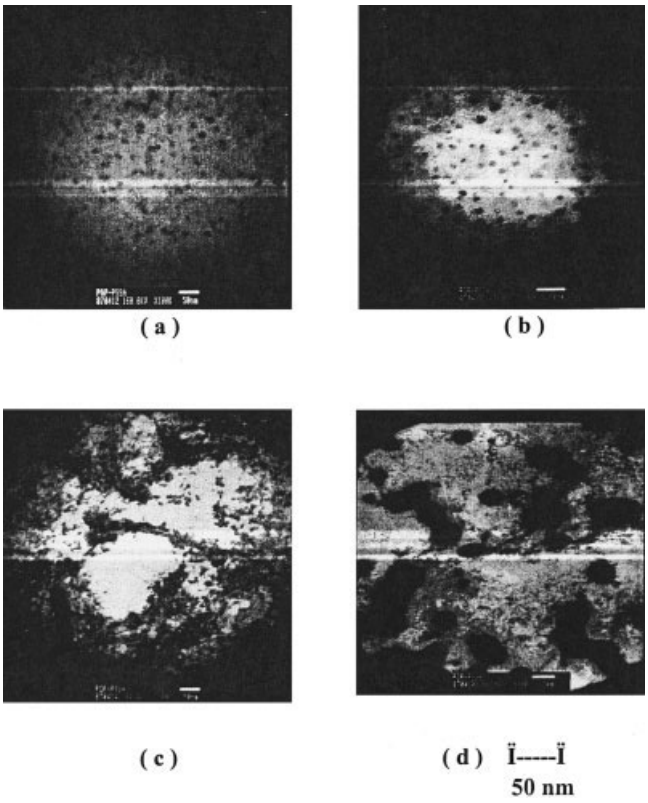

Figure 14 TEM micrographs of POP–PSSA complexes [160 kV; (a) ×120,000; (b) ×150,000; (c) ×200,000; (d) ×100,000].

the W═O terminal stretching vibration peak (~980 cm^{-1}).[29] Figure 11 shows the SEM micrograph of PANI–PSSA by electrochemical polymerization on ITO surface has a globular structure.

WO_3 film

The physical and chemical properties of electro-deposited film obtained from aqueous solution containing tungsten and hydrogen peroxide (30%, R.D.H) depended strongly on the solution composition. When the hydrogen peroxide content in the solutions was high, the electro-deposition efficiency under a constant current was low, possibly because the oxidation atmosphere in the solutions was too strong.[61] In this case, colorless thin films (WO_3) were obtained.

A blue electro-deposited film changed into a colorless film upon a heat treatment above 140°C (1 h). This is considered to be due to the reaction of tungsten bronze to tungsten oxide, as presented in eq. (1)[61]:

$$H_xWO_{3-\delta}\cdot H_2O \xrightarrow{heat} WO_{3-\delta}(1 + 0.5x - n)H_2O + nH_2O\text{Blue} > 140^\circ\text{C(1h) colorless} \quad (1)$$

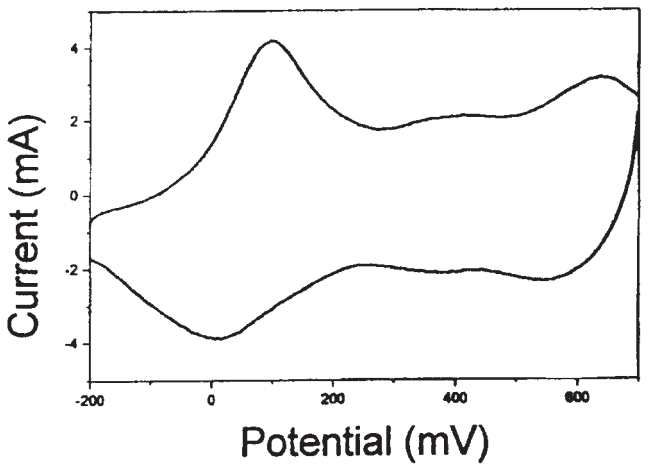

Figure 15 Cyclic voltammograms of the PANI on ITO.

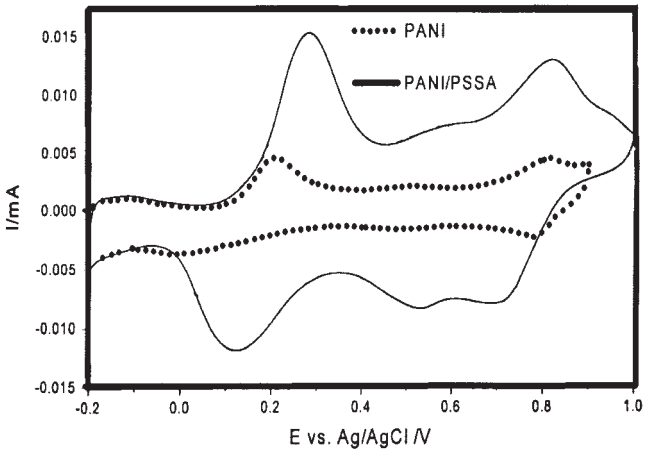

Figure 16 Cyclic voltammograms of the PANI–PSSA/PANI on the ITO.

Devices

Device 1: glass/ITO/PANI-PSSA/PAMPSA/WO_3/ITO/glass. The device window was cycled, and only a blue color could be observed at high positive potentials; at negative potentials the device was still turning transparent. However, after applying a constant potential of +3000 mV for 5 min, the device regained its dark blue color.

Device 2: glass/ITO/PANI-PSSA/PAMPSA/ITO/glass. The cyclic voltammograms had almost no current response with no color change, as for device 1, configuration color time had increased to 10 min, i.e., by applying a constant potential of +3000 mV for 10 min, the device regained its blue color. Table VIII summarizes some of the characteristics data for the two device configurations, device 1 and device 2, and shows some of the noteworthy characteristics of conducting polymers and electrochromic device effectiveness.[47] The positive voltage means that PANI–PSSA is oxidized and WO_3 is reduced, and the window obtains a

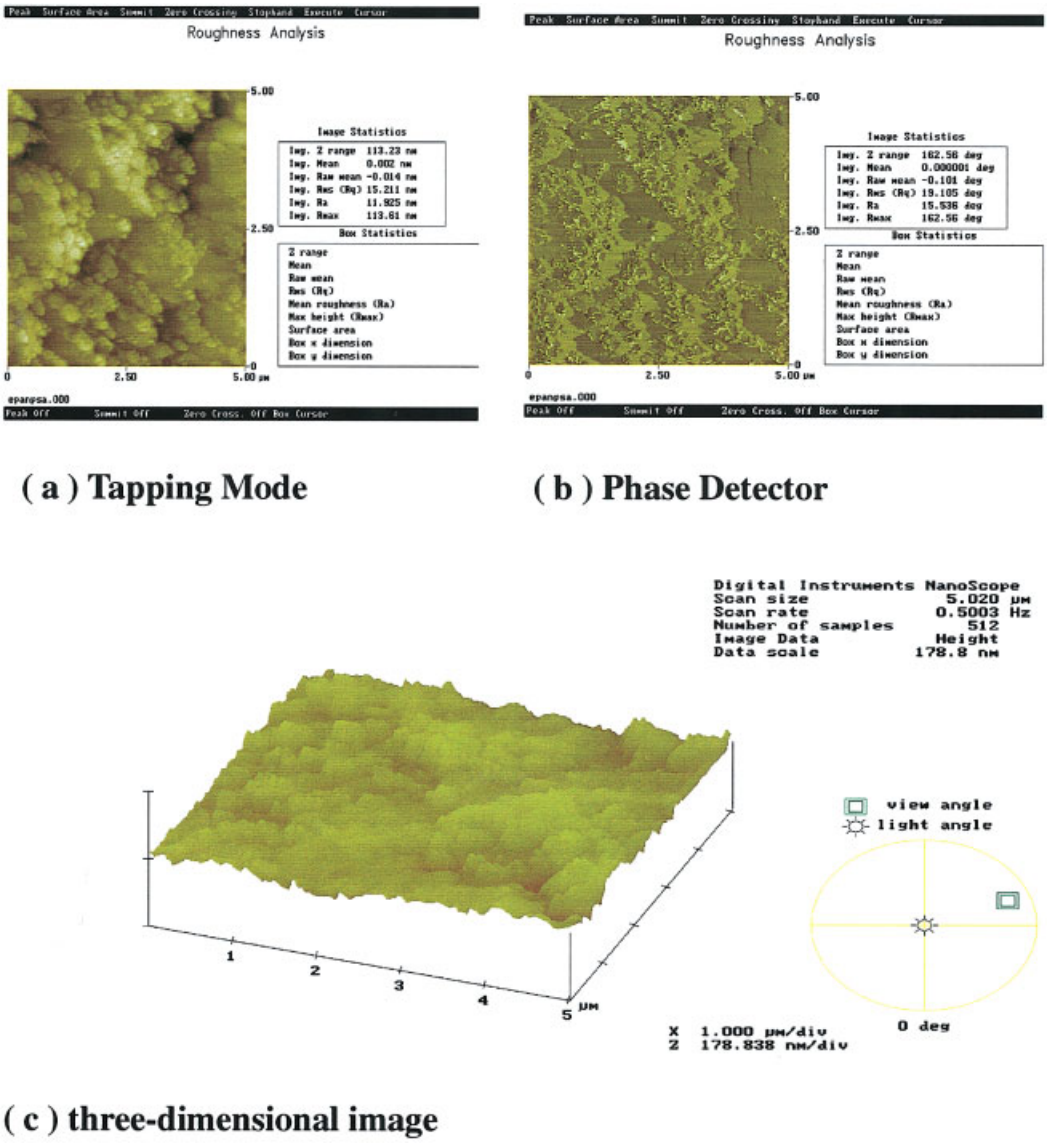

Figure 17 AFM topography of PANI–PSSA blend on ITO: (a) tapping model without phase detector, (b) tapping model with a phase detector, and (c) a three-dimensional image. [Color figure can be viewed in the online issue, which is available at www.interscience.wiley.com.]

blue color. By cycling between −3000 and +3000 mV, the color switches from almost transparent to dark blue, respectively. Application of higher potentials, (i.e., up to +3500 mV), results in a violet color, which indicate irreversible degradation of PANI–PSSA. Cyclic votammograms (50 mV/s) of the two device configurations, in the potential region from –3000 to +3000 mV, are shown in Figures 20 and 21. The change in absorption obtained proves that the tungsten trioxide electrode concept is valid. These contrasts are insufficient (50%, at 720 nm), and these films have very good electro-chromic efficiency at 720 nm.

Color and discolor

The electrochromic window with PANI–PSSA[58] and WO_3[43] electrochemically deposited on indium-tinoxide (ITO) coated glass plates and with poly(2-acrylamido-2-methyl propane-sulfonic acid) (PAMPSA) as a solid organic polymer electrolyte.[20] The total glass sandwich becomes Glass/ITO/PANI–PSSA/PAMPSA/WO_3/ITO/Glass, the schematic cell reaction in the window also indicating the color changes, and can be written as[34]:

$$\underset{\text{(Green)}}{\text{PANI-PSSA}^{n}} \leftrightarrow \underset{\text{(Blue)}}{(\text{PANI-PSSA})^{x+n}} + xe^{-} \quad (2)$$

$$\underset{\text{(Colorless)}}{WO_3} + xM^{+} + xe^{-} \leftrightarrow \underset{\text{(Blue)}}{MxWO_3} \quad (3)$$

where x is the number of cation (M^+, for example: H^+ that from PAMPSA ([sbond]$SO_3^-H^+$), or PSSA

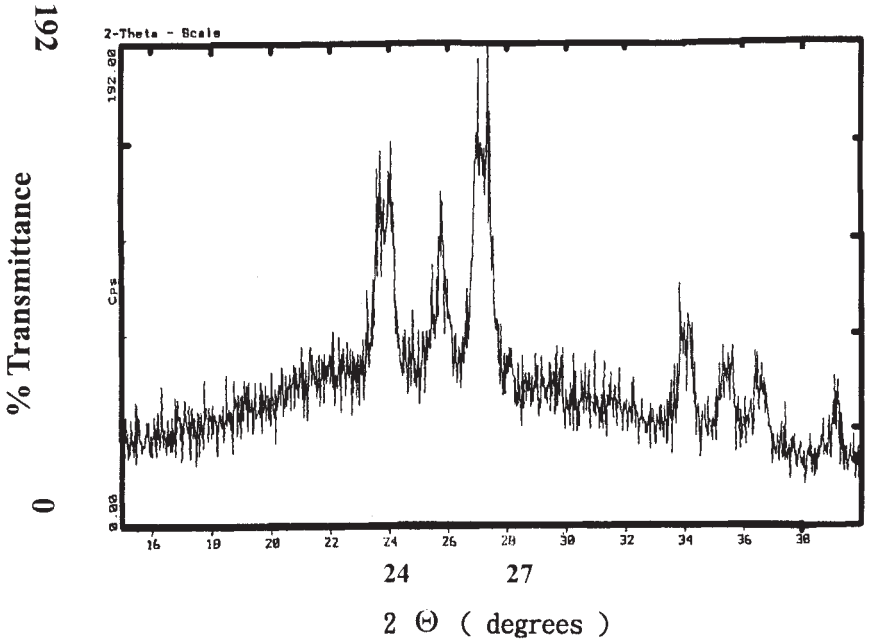

Figure 18 XRD spectrum of the WO_3 compound.

([sbond]$SO_3^-H^+$), or H_2O; if have) and anions (A^-, for example : Cl^-) transferred in the reaction; n is the oxidation state of PANI–PSSA. Those cell reactions (2) and (3) are oversimplified, and do not include the necessary proton transfer in PANI–PSSA during the red-ox process. The degree of light modulation in the 200–900 nm region by applying a voltage between −3000 and +3000 mV is found (Figs. 20 and 21) to be quite good, for example: a change in absorbance from 1.2 (−3000 mV) to 0.6 (+2500 mV) at 720 nm.

Cyclic voltammograms (50 mV/s) of the PANI, POP, and P2E on ITO, in the potential region −200 to +700 mV, are shown in Figures 22, 23, and 24. Cyclic voltammograms (50 mV/s) of the PANI–PSSA, POP–PSSA, and P2E–PSSA on ITO, in the potential region –200 to +800 mV, are shown in Figures 25–27. There are two oxidation state peaks shown polyaniline peak characters is near 0.5 and 0.3 V, respectively. In the anodic sweep, three major redox couples are distinguishable (the first, formation of radical cations peak (polaromic emeraldine); the second, formation of benzoquinone peak, and the third, formation of diradicals dications),[62] commences at ~600 mV, and reaches a maximum at 800 mV. In the cathodic sweep, the presence of three corresponding broad reduction peaks. A comparison of the cyclic voltammgrams of PANI–

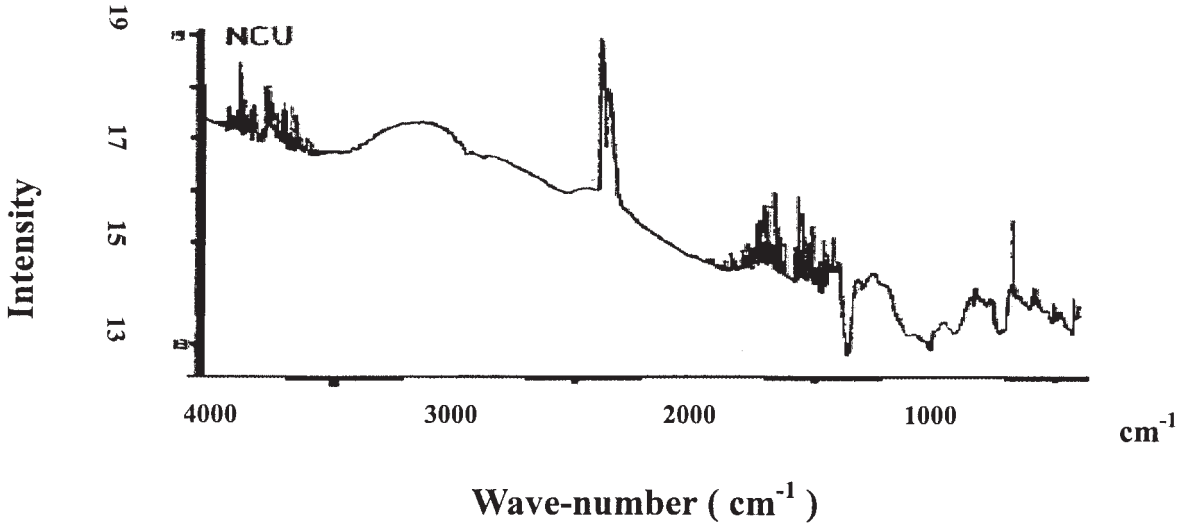

Figure 19 IR spectrum of the WO_3.

TABLE VIII
Characteristics Data for the Two Device Configurations with and without WO_3 Data are Given for Discolor/Color

Device	Device 1[a]	Device 2[b]
Size (cm^2)	2	2
Color	Transparent/blue	Transparent/blue
Voltage (V)	>3	>3
Current ($\mu A/cm^2$)	$<10^{-3}$	$<10^{-3}$
Absorbance (720 nm)	1.2 → 0.6	1.0 → 0.6

[a] Device 1: Glass/ITO/PANI–PSSA/PAMPSA/WO_3/ITO/Glass.
[b] Device 2: Glass/ITO/PANI–PSSA/PAMPSA/ITO/Glass.

PSSA and PANI, POP–PSSA and POP, P2E–PSSA and P2E, respectively,; the two oxidation peaks of PANI–PSSA, POP–PSSA, and P2E–PSSA is with much stronger and close than that observed in PANI, P2E and POP, respectively, suggests PSSA having the template effect; and the two oxidation peaks of POP–PSSA and P2E–PSSA is much more closer than that observed in PANI–PSSA, also suggests the reactivity of side group chains —OC_2H_5 and —C_2H_5.

The SEM and AFM micorgraphy of the substituted polyaniline salts and their complexes by electrochemical polymerization on ITO shown in Figures 11, 17, 28, and 29, the surface morphology of the substituted ployaniline complexes and their salts is globular structure.

Under the same film thickness

The best color and discolor time of the polyniline–poly(styrenesulfonic acid), poly(2-ethylaniline)-poly(styrenesulfonic acid) and poly(o-phenetidine)–poly(styrenesulfonic acid). A film thickness of 10 μm was chosen and estimated from the charge crossing the electrolytic cell. Average film growing rate of the PANI–PSSA (Fig. 30), POP–PSSA (Fig. 31), and P2E–PSSA (Fig. 32) complexes is 0.54, 1.00, and 0.79 μm/s, respectively. The best color and discolor time of PANI–PSSA is slower than those of POP–PSSA (500/250 ms) and P2E–PSSA (750/500 ms) complexes, respectively. The PANI–PSSA complexes film thickness is smaller than POP–PSSA and P2E–PSSA complexes, i.e., the reactivity of *o*-phenetidine and 2-ethylaniline is larger than that of aniline.

Under the same reaction time and same monomer concentration

The best color and discolor time of polyaniline–poly(styrenesulfonic acid) [PANI–PSSA], poly(o-phenetidine)–poly-(styrenesulfonic acid) [POP–PSSA] and poly(2-ethylaniline)–poly(styrenesulfonic acid)[P2E–PSSA] complexes. The electrochemical polymerization film thickness of PANI–PSSA, POP–PSSA, and P2E–PSSA complexes is shown in Table IX. Under same reaction concentration and same reaction time of 3 s, the average color and discolor time of POP–PSSA is 175/150 ms; the best color and discolor time of POP–PSSA is 125/125 ms. POP–PSSA and P2E–PSSA are faster than PANI–PSSA.

Under the same reaction concentration and reaction time of 10 s, the average color and discolor time of POP–PSSA and P2E–PSSA measured are 322/288 ms and 719/563 ms, respectively, and are faster than that of PANI–PSSA. The best color and discolor time of POP–PSSA and P2E–PSSA is measured as 250/200 and 625/500 ms, shown in Table X, respectively, and are faster than PANI–PSSA. Under both the same reaction concentration and same reaction time, 25 s, average color and discolor time of POP–PSSA is 1005/808 ms. The best color and discolor time of POP–PSSA is 550/375 ms; and are faster than that of PANI–PSSA. The electrochemical polymerization of POP–PSSA and PANI–PSSA on ITO, the film thickness is more heavy, the color and discolor response time is longer. POP–PSSA not only presence of electro-donating (—OC_2H_5) group present in aniline monomer but also induce effect by the alkyl group (—OC_2H_5), and the —SO_3H group on the polyelectrolyte, which let the color and discolor time be shorter.

Under the same film thickness, both the same reaction time and same monomer concentration, check the results in hydrochloride acid, the substituted polyaniline due to presence of electro-donating (—C_2H_5 or

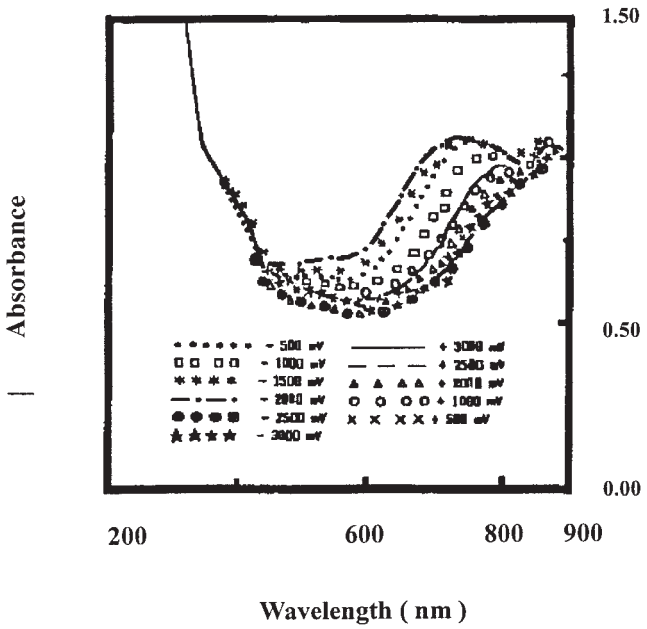

Figure 20 Absorbance versus wavelength in the electrochromic window glass/ITO/PANI–PSSA/PAMPSA/ITO/glass at different applied potentials.

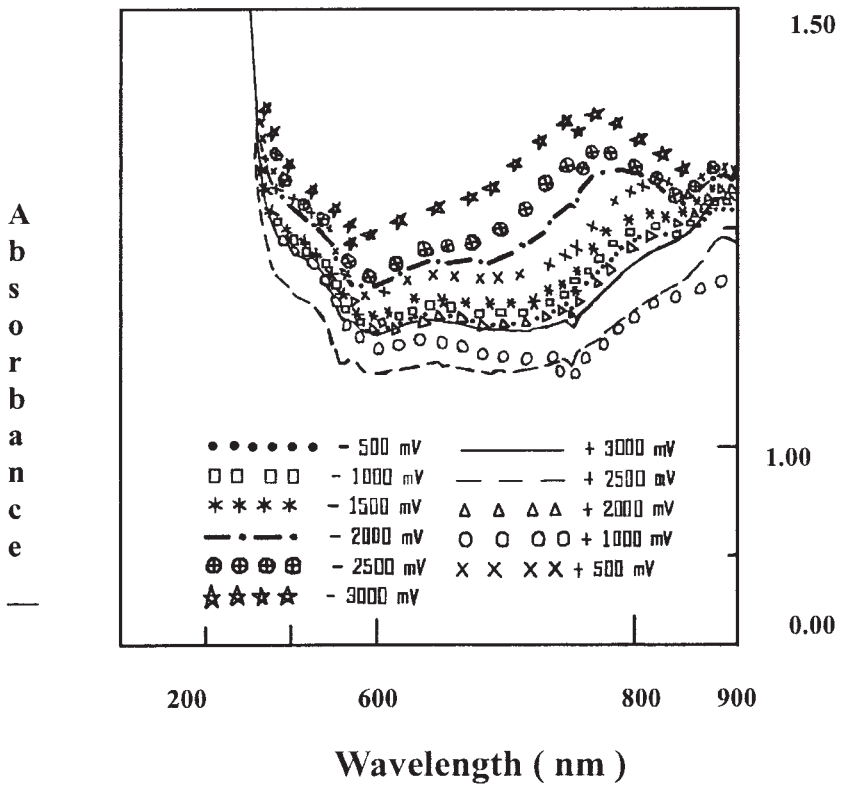

Figure 21 Absorbance versus wavelength in the electro-chromic window glass/ITO/PANI–PSSA/PAMPSA/WO_3/ITO/glass at different applied potentials.

—OC_2H_5) group present in aniline monomer, to form a network structure, both the surface with much porous, and ion transfer easy, conductivity easy, so with short the color and discolor time. For *o*-phenetidine, both monomer reactivity and due to presence of electro-donating (—OC_2H_5) group present in aniline monomer, let the substituted polyaniline have much short chain, so with shorter color and discolor time.

The side chain group of —OC_2H_5 and —C_2H_5 groups are electron-donating group, not only the presence of electro-donating(—OC_2H_5) group present in aniline monomer but also the —OC_2H_5 group having induce effect; and —C_2H_5 group only presence of electro-donating (—C_2H_5) group present in aniline monomer. Relativity to the electrochemical polymerization reactivity of monomer (aniline, *o*-phenetidine,

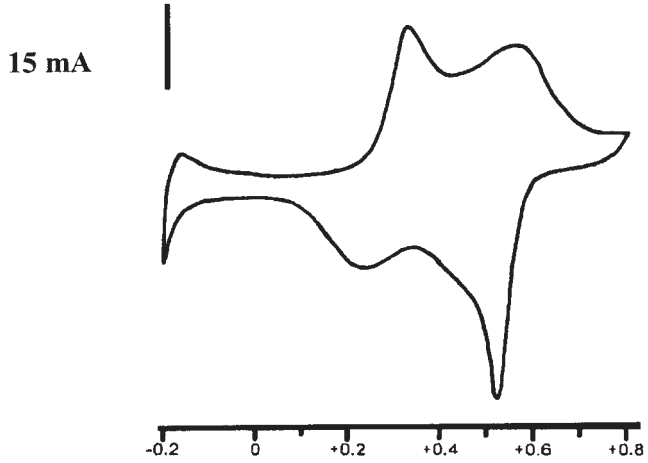

Figure 22 Cyclic voltammogram for the electrochemical synthesized thin PANI film in 0.2*M* aniline (scan rate: 50 mV/s).

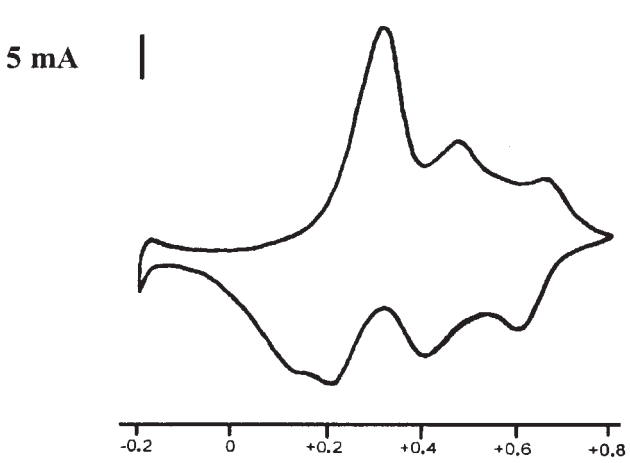

Figure 23 Cyclic voltammogram for the electrochemical synthesized thin POP film in 0.2*M* *o*-phenetidine (scan rate: 50 mV/s).

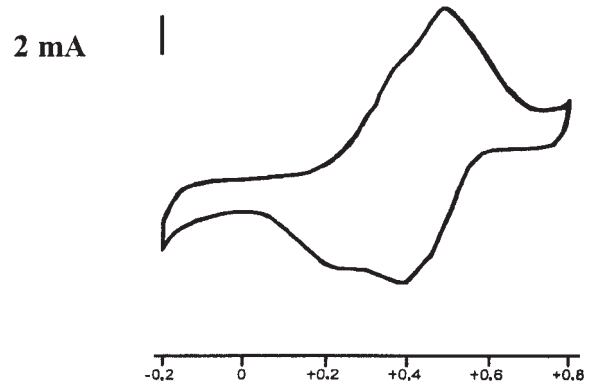

Figure 24 Cyclic voltammogram for the electrochemical synthesized thin P2E film in 0.2*M* 2-ethylaniline (scan rate: 50 mV/s).

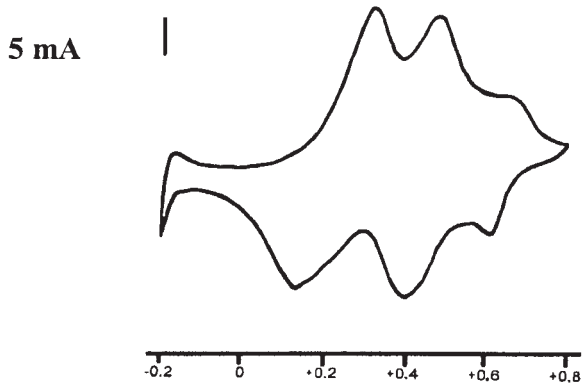

Figure 26 Cyclic voltammogram for the electrochemical synthesized thin POP–PSSA film in 0.2*M* *o*-phenetidine with 0.2*M* PSSA (scan rate: 50 mV/s).

or 2-ethylaniline) with PSSA, the film growing rate of PANI–PSSA is smaller than that of POP–PSSA and P2E–PSSA, PANI–PSSA is the lowest. During the electrochemical process that relatively to the oxidation potential of PANI–PSSA is higher, P2E–PSSA and POP–PSSA is the lower, and the oxidation reversibility of POP–PSSA and P2E–PSSA is larger than that of PANI–PSSA.

Ambient temperature conductivity

The EPR spectra of all substituted polyaniline salts and their complexes shows a single Lorentzian shaped signal without any hyperfine splitting (Fig. 9). The electrical conductivity of PANI–PSSA (4.7×10^{-2} S/cm) is higher than those of P2E–PSSA (2.4×10^{-2} S/cm) and POP–PSSA (3.8×10^{-2} S/cm), which suggests that the side group (—C_2H_5, or —OC_2H_5) has a definite influence on the polymer chain.

Low-temperature EPR spectra

Temperature-dependent EPR studies were performed at 298 K and 77 K. Tables VI and VII, show the results of EPR spectra of all substituted polyaniline HCl salts and substituted polyaniline-polyelectrolyte complexes in argon and air, respectively. The g values are around 2.00290–2.00321, which are almost the free-electron *g* value, and this suggests that polyaniline exists primarily as the polysemiquinone radical cation.

The line-width of the substituted polyaniline complexes are rather small (1.626 G–5.448 G) compared with those of the substituted polyaniline salts (2.270 G–12.227 G), where the dominant broadening mechanism is the hyperfine interaction with adjacent protons.

Factors influencing EPR line-width

The electrical conductivity (i.e., line width) of substituted polyaniline HCl salts and their complexes de-

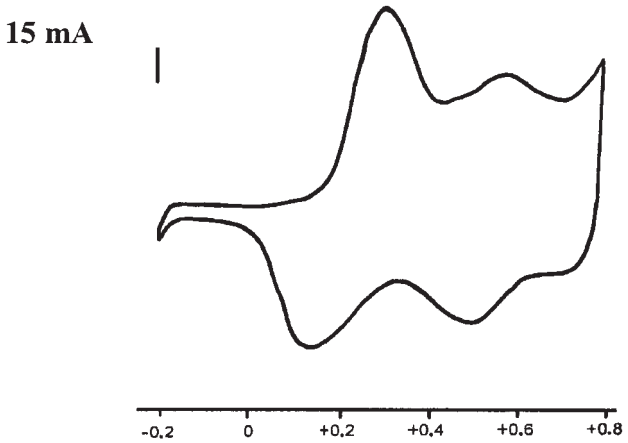

Figure 25 Cyclic voltammogram for the electrochemical synthesized thin PANI–PSSA film in 0.2*M* aniline with 0.2*M* PSSA (scan rate: 50 mV/s).

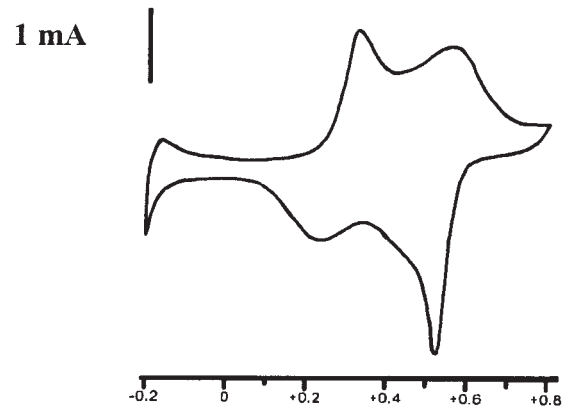

Figure 27 Cyclic voltammogram for the electrochemical synthesized thin P2E–PSSA film in 0.2*M* 2-ethylaniline with 0.2*M* PSSA (scan rate: 50 mV/s).

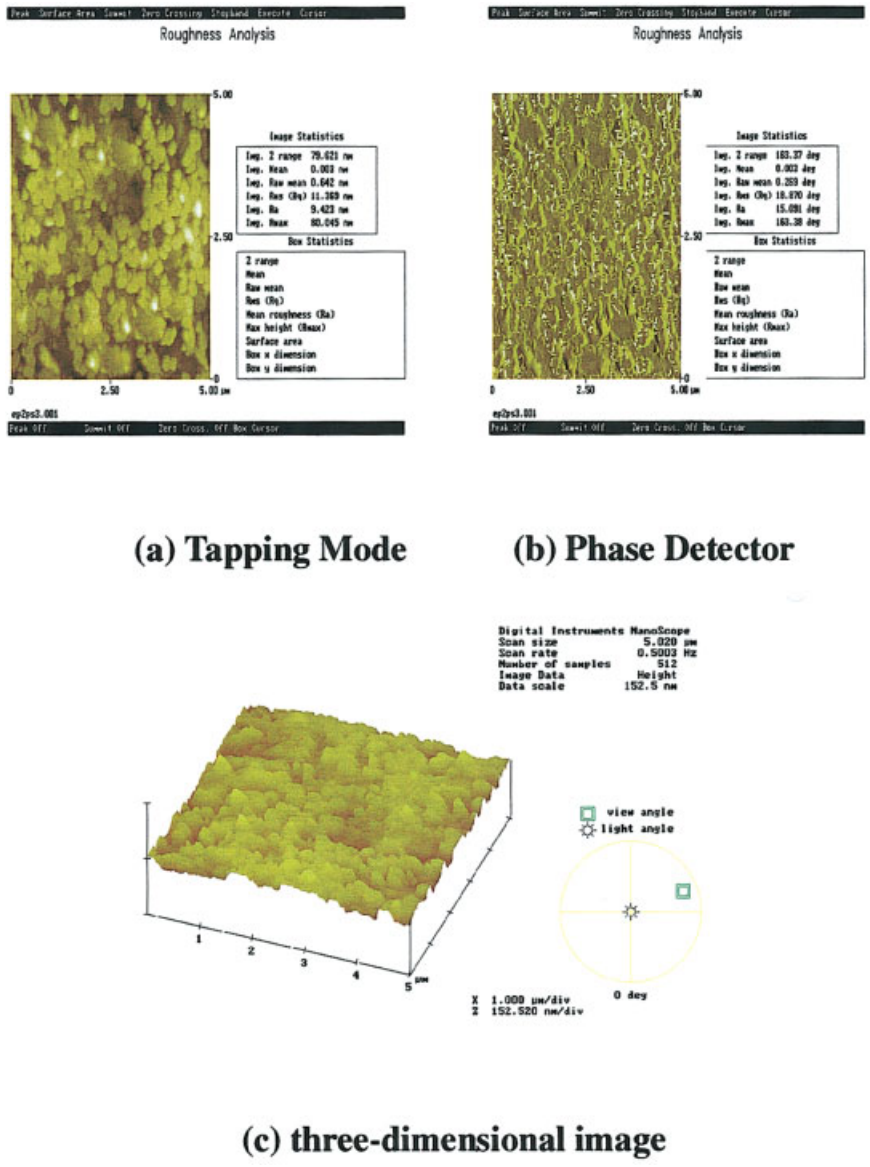

Figure 28 AFM topography of P2E–PSSA blend on ITO: (a) tapping model without phase detector, (b) tapping model with a phase detector, and (c) a three-dimensional image. [Color figure can be viewed in the online issue, which is available at www.interscience.wiley.com.]

creased upon exposure to oxygen and increased reversibly in argon. The narrower line-widths of unsubstituted and substituted polyaniline complexes compared with those or HCl salts can be attributed to the lower degree of structural disorder. The conductivity of the unsubstituted and substituted polyaniline polyelectrolyte system is low due to localization, since they are heavily doped and lower disordered systems. The electron localization in the P2E–PSSA and POP–PSSA is greater than PANI–PSSA, the electron-donating character of the ethyl group and ethoxy group appears to reduce conductivity.

Relationship of EPR to conductivity

The conductivity of the PANI–PSSA, P2E–PSSA, and POP–PSSA are around 10^{-2} S/cm, EPR spectral data give evidence for the existence of highly mobile radical cations or polarons of the substituted polyaniline salts as well as their complexes, is shown to be due to localization since they are heavily doped and lower disordered systems.

CONCLUSIONS

We have prepared polyaniline polyelectrolyte complexes PANI–PSSA, POP–PSSA, and P2E–PSSA. IR spectra absorption bands are at ~1600 cm^{-1} (C═C stretching in quionoid unit), ~1500 cm^{-1} (C═C stretching in benzenoid unit), 1200, 1040, and 1020 cm^{-1}(—SO_3H), 1100 cm^{-1}(aromatic C—O stretching), and at 930–800 and 770–750 cm^{-1} (1,2,4-trisubstituted phenyl ring); show that PANI–PSSA, P2E–PSSA, and

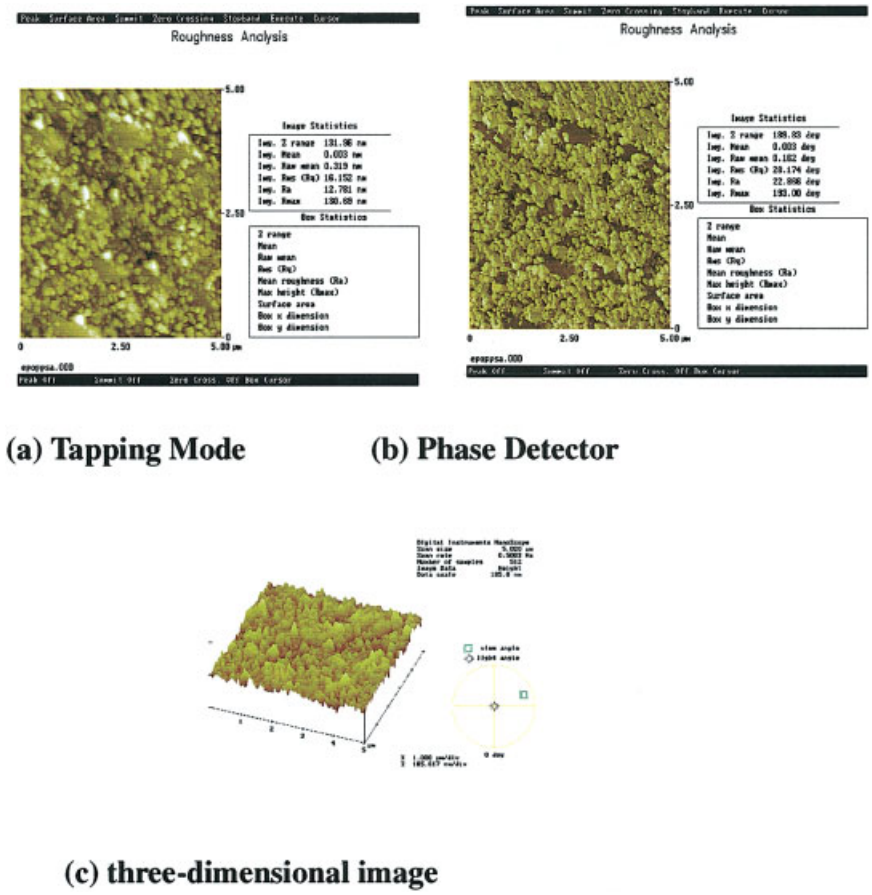

Figure 29 AFM topography of POP–PSSA blend on ITO: (a) tapping model without phase detector,(b) tapping model with a phase detector, and (c) a three-dimensional image. [Color figure can be viewed in the online issue, which is available at www.interscience.wiley.com.]

POP–PSSA complexes have structures similar to those of the unsubstitued polyaniline. After deprotonation with base [PANI–PSSA (pH ≥ 10.0); POP–PSSA (pH ≥ 8.0); P2E–PSSA (pH ≥ 9.5)], a peak at ~580 nm appears. The pH value for deprotonation is higher than that of HCl salt of polyaniline. The results indicate an intimate interaction between the two polymer chains, products with good water solubility [3.1 g/L for PANI–PSSA, 2.9 g/L for P2E–PSSA, and 1.9 g/L for POP–PSSA] have been obtained. EPR and VIS spectra indicate the formation of polarons. Elemental analysis shown that PANI–PSSA has a high nitrogen to sulfur ratio (N/S) of 38%, lower than that for P2E–PSSA (41%) and POP–PSSA(52%). The conductivity of PANI–PSSA, POP–PSSA, and P2E–PSSA are around 10^{-2} S/cm; low conductivity due to localization, heavily doped and lower disordered.

Temperature-dependent transport properties suggest that all polyaniline complexes have a single fine signal without any hyperfine splitting structure. The g value of all the salts and complexes are between 2.00290–2.00321, which is almost the free-electron g

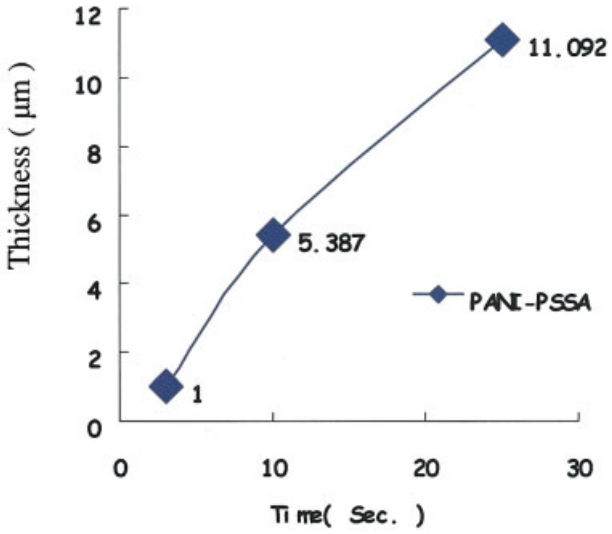

Figure 30 Film growing rate of polyaniline–poly(styrenesulfonic acid)[PANI–PSSA] complexes. [Color figure can be viewed in the online issue, which is available at www.interscience.wiley.com.]

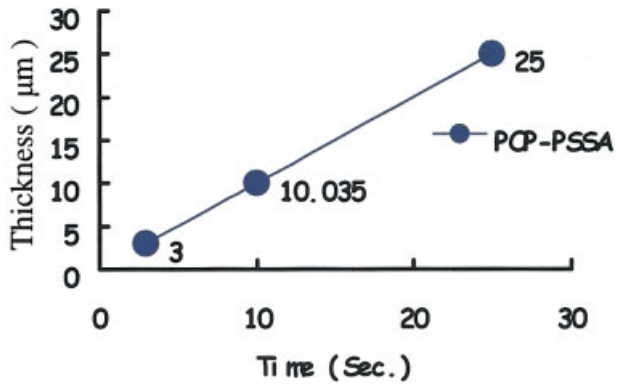

Figure 31 Film growing rate of poly(*o*-phenetidine)–poly-(styrenesulfonic acid)[POP–PSSA] complexes. [Color figure can be viewed in the online issue, which is available at www.interscience.wiley.com.]

value. The narrower line-widths of PANI–PSSA, POP–PSSA, and P2E–PSSA complexes can be attributed to the lower degree of structural disorder. The presence of electro-donating (—OC_2H_5, or —C_2H_5) group present in aniline monomer, decreasing the degree of delocalization of the radical cation, the side group ethyl- or ethoxy-group appears to reduce the conductivity, the presence of excessive —SO_3— lead primarily to the formation of bipolarons, and thus to a lower conductivity.

The SEM micrographs show the surface morphology of the PANI–PSSA has a globular structure, POP–PSSA is a film with porous structure, and P2E–PSSA has globular irregular structure. The POP–PSSA complexes, measured by TEM, shown as the particulates of poly(*o*-phenetidine) in complexes reacted with poly(styrenesulfonic acid) polyelectrolyte crosslink subsequent to form a channel, useful for the electron transfer.

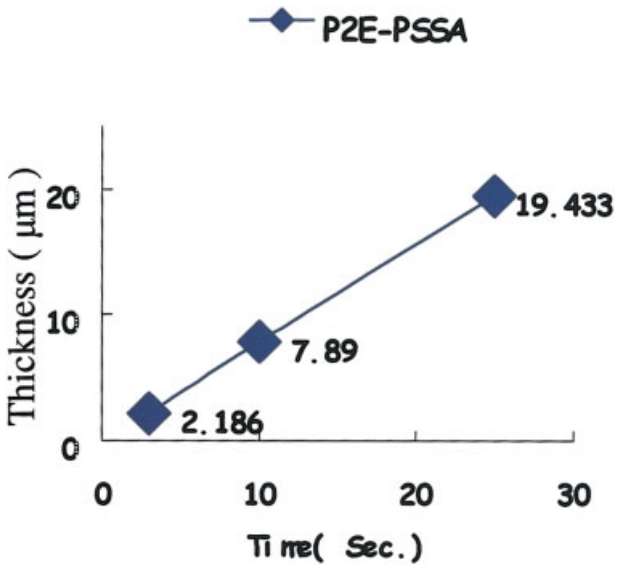

Figure 32 Film growing rate of poly(2-ethylaniline)–poly-(styrenesulfonic acid)[P2E–PSSA]complexes. [Color figure can be viewed in the online issue, which is available at www.interscience.wiley.com.]

TABLE IX
Film Thickness of Poly(*o*-anisidine)–Poly(styrene sulfonic acid) [POA–PSSA], Poly(*o*-phenetidine)–Poly(styrenesulfonic acid) [POP–PSSA], Poly(2-ethylaniline)–Poly(styrenesulfonic acid) P2E–PSSA], and Polyaniline–Poly(styrenesulfonic acid) [PANI–PSSA] in a Various Reaction Time

Sample	Reaction time (s)	Film thickness (μm)	Average film growing rate (μm/s)
POA–PSSA	3	4.13	
	10	12.31	
	25	>25	
	60	>25	≧1.20
POP–PSSA	3	3	
	10	10.04	
	25	25	
	60	>25	1.00
P2E–PSSA	3	2.19	
	10	7.89	
	25	19.43	
	60	25	
	120	>25	≧0.79
PANI–PSSA	3	1.00	
	10	5.39	
	25	11.09	
	60	11.53	
	120	>25	≦0.54

Film thickness is the average of 5 times of measurement by Nanospectrometer.

An electrochromic device consisting of polyaniline–poly(styrenesulfonic acid) [PANI–PSSA], tungsten oxide(WO_3), the solid polymer electrolyte poly(2-acrylamido-2-methylpropane-sulfonic acid) [PAMPSA], and glass plates coated with indium-tin oxide (ITO) show good properties for light modulation in the 200–900 nm wavelength region. By changing the applied voltage from +3000 mV, the absorption is shifted from 1.20 to 0.60 at 720 nm.

The results of electrochemical response time of the substituted polyaniline complexes are described as the following conditions. First, Under same reaction time of 3 s, both monomer (aniline, *o*-phenetidine, or 2-ethylaniline) concentrations are 0.6*M* with poly(styrenesulfonic acid) concentration is 0.15*M*, the best color and discolor time (film thickness) of poly(2-ethylaniline)-poly(styrenesulfonic acid) is 500/300 ms (2.19 μm); poly(*o*-phenetidine)–poly(styrenesulfonic acid) complexes is 125/125 ms (3.00 μm), the results are attributed to the substituted polyaniline due to presence of electro-donating (—OC_2H_5 or —C_2H_5,) group present in aniline monomer, which let color and discolor time of poly(*o*-phenetidine)–poly(styrenesulfonic acid) and poly(2-ethylaniline)–poly(styrenesulfonic acid) are faster than polyaniline–poly(styrenesulfonic acid). Secondly, Under the same film thickness

TABLE X
The Best Color and Discolor Time of Poly(*o*-anisidine)–Poly(styrenesulfonic acid) [POA–PSSA], Poly(*o*-phenetidine)–Poly(styrenesulfonic acid) [POP–PSSA], and Poly(2-ethylaniline)–Poly(styrenesulfonic acid) [P2E–PSSA] Complexes by Electrochemical Polymerization

Reaction time (s)	Sample	Substituted group	Color time (ms)	Discolor time (ms)	Film thickness (μm)
3	POA–PSSA	—OCH_3	125	125	4.13
	POP–PSSA	—OC_2H_5	125	125	3.00
	P2E–PSSA	—C_2H_5	500	300	2.19
10	POA–PSSA	—OCH_3	250	320	12.31
	POP–PSSA	—OC_2H_5	250	200	10.04
	P2E–PSSA	—C_2H_5	625	500	7.89
25	POA–PSSA	—OCH_3	875	750	$\gg$25
	POP–PSSA	—OC_2H_5	550	375	$>$25

The film thickness is the average of 5 times for measurement by Nanospectrometer.

(10 μm), electrochemical polymerization on the concentration of the poly(styrenesulfonic acid) is 0.15*M*, with monomer (reaction time) [aniline(18.5 s), *o*-phentidine(10 s), or 2-ethylaniline (12.7 s)] concentration is 0.6*M*, the best color and discolor time of polyaniline–poly(styrenesulfonic acid) is 1500/750 ms; poly(*o*-phenetidine)–poly(styrenesulfonic acid) is 500/250 ms; poly(2-ethylaniline)–ply(styrenesulfonic acid) is 750/500 ms. The ploly(*o*-phenetidine)–poly(styrenesulfonic acid) and poly(2-ethylaniline)–ply(styrenesulfonic acid) are much faster than polyaniline–poly(styrenesulfonic acid). Third, Film growing rate of polyaniline–poly(styrenesulfonic acid) [0.54 μm/s] is slower than that of poly(*o*-phenetidine)–poly(styrenesulfonic acid)[1.00 μm/s] and poly(2-ethylaniline)–poly(styrenesulfonic acid) [0.79 μm/s]. From the surface morphology, the porous density of the poly(*o*-phenetidine)–poly(styrenesulfonic acid) and poly(2-ethylaniline)–poly(styrenesulfonic acid) are much rich than those of polyaniline–poly(styrenesulfonic acid) complexes, is very easy for proton and ion transfer, color and discolor time is change very large. In substituted polyaniline structure, because of presence of electro-donating (—OC_2H_5 or —C_2H_5,) group present in aniline monomer, the bigger group (—OC_2H_5), both larger reactivity and much porous, is very useful for proton or ion transfer.

The PANI–PSSA, POP–PSSA, and P2E–PSSA complexes show a single fine signal without any hyperfine splitting structure. The *g* values are around 2.00290–2.00321, which is almost the free-electron g value. The narrower line width in polyaniline complexes compared with that of HCl salts can be attributed to the lower degree of structural disorder. Larger line width of the substituted polyaniline complexes can be attributed to the presence of electro-donating (—OC_2H_5 or —C_2H_5,) group present in aniline monomer that decreasing the degree of delocalization of radical cation. The electron-donating character of the ethyl group and ethoxy group appears to reduce conductivity. The addition of side chain groups (—C_2H_5 or —OC_2H_5) and the presence of excessive —SO_3^- lead primarily to the formation of bipolarons, and thus, lower conductivity, because of localization since they are heavily doped and lower disordered systems. We conclude, therefore, that while the magnetic properties are due to polaron spins, both the paramagnetic polarons (radical cations) and the diamagnetic bipolarons (spinless; dications) are involved in the charge transport.

Professor S. C. Yang of Rhode Island University, USA. Professors Chemg-Heng Kao, Chun-Guey Wu, Shin-Shing Shyu, Wen-Yih Chen, Anthony S.T. Chiang, Chin-Hang Shu, Hsiao-Tsung Lin, Hui Chen, Liang-Sun Lee, Ten-Tsai Wang, Yin-Zu Chen, George Ting-Kuo Fey, Louis Loung-Yie Tsai, Show-jane Hsieh of the National Central University, Professor Lee Y. Wang and Tsu-Ming Pan of the National Taiwan University, Professor Tian-Chyuan Huang of the National Taipei college Nursing, Professor Mei-chun Lin (Dept. de Francais) of the Chinese Culture University, Professor. Hsi-Hwa Tso and Tein-Fu Wang (Institute of Chemistry, Academia Sinica), Professor Hsing-Wen Sung and Kuei-jung Chao of the National Tsing Hua University, Professors Kan-Nan Chen, Wen-Jwu Wang, Bo-Cheng Wang of the Tamkang University, Professor F.-M. Pan of the National Nano Device Lab., Hsiu-hsen Yao of the Yuan-Ze University, Dr. Hideki Shirakawa (Professor Emeritus, University of Tsukuba, Japan) and prof. Arthur J. Epstein (The Ohio State University, Dept. of Physics) is also acknowledged.

References

1. Lampert, C. M. Sol Energy Mater Sol Cells 1984, 11, 1.
2. Lampert, C. M. Sol Energy Mater Sol Cells 1998, 55, 301.
3. Ozer, N.; Lampert, C. M. Sol Energy Mater Sol Cells 1998, 54, 147.
4. Lampert, C. M. Sol Energy Mater Sol Cells 1994, 33, 389.
5. Osaka, T.; Ogano, S.; Naoi, K. J Electrochem Soc 1989, 136, 306.
6. Somasini, N. L. D.; MacDiarmid, A. G. J Appl Electrochem 1988, 18, 92.
7. Goto, F.; Okabayashi, K.; Yoshida, T.; Morimoto, H. J Power Sources 1987, 20, 243.
8. Noufi, R.; Nozik, A. J.; White, J.; Warren, L. F. J Electrochem Soc 1982, 129, 226.

9. Josowiaz, M.; Janata, J. J Anal Chem 1986, 58, 514.
10. Bull, R. A.; Fan, F. R.; Bard, A. J. J Electrochem Soc 1984, 131, 687.
11. Heinze, J. Synth Met 1991, 41, 2805.
12. Zoppi, R. A.; De Paoli, M. A. Quim Nova 1993, 16, 560.
13. Scrosati, B. In Applications of Electroactive Polymers; Scrosati, B., Ed.; Chapman & Hall: London, 1993; p 267.
14. Svensson, J. S. E. M.; Granqvist, C. G. Thin Solid Films 1985, 126, 31.
15. Goldner, R. B.; Haas, T. E.; Seward, G.; Wong, K. K.; Norton, P.; Foley, G.; Berera, G.; Wei, G.; Schulz, S.; Chapman, R. Solid State Ionics 1988, 28, 1715.
16. Nguyen, M. T.; Dao, L. H. J Electrochem Soc 1989, 136, 2131.
17. Dao, L. H.; Nguyen, M. T. In Electrochromic Materials. The Electrochemical Society Soft Bound Proceedings Series; The Electrochemical Society: Pennington, New Jersey, 1990; p 246.
18. Yang, S. C. Large-area Chromogenics: Materials and Devices for Transmittance Control; Lampert, C. M., Granqvist, C. G., Ed.; SPIE Press: Washington, 1990; p 335.
19. Hyodo, K. Electrochim Acta 1994, 39, 265.
20. Jelle, B. P.; Hagen, G.; Odegard, R. Electrochim Acta 1992, 37, 1377.
21. Jelle, B. P.; Hagen, G. J Electrochem Soc 1993, 140, 3560.
22. Jelle, B. P.; Hagen, G.; Hesjevik, S. M.; Odegard, R. Mater Sci Eng B 1992, 13, 239.
23. Jelle, B. P.; Hagen, G.; Sunde, S.; Odegard, R. Synth Met 1993, 54, 315.
24. Liu, J. M.; Yang, S. C. J Chem Soc Chem Commun 1991, 1529.
25. Faughnan, B. W.; Crandall, R. S.; Heyman, P. M. RCA Rev 1975, 36, 177.
26. Mohapatra, S. K. J Electrochem Soc 1978, 125, 284.
27. Yamanaka, K. J. J Appl Phys 1986, 25, 1073.
28. Zeller, H. Z.; Beyeler, H. U. Appl Phys 1977, 13, 231.
29. Ohsawa, T.; Kabata, T.; Kimura, O. Synth Met 1989, 29, E203.
30. Stevens, J. R.; Sevensson, J. S. E. M.; Granqvist, C. G.; Spinder, R. Appl Opt 1987, 26, 3489.
31. Angelopoulos, M.; Dipietro, R.; Zheng, W. G.; MacDiarmid, A. G.; Epstein, A. J. Synth Met 1997, 84, 35.
32. Jozefowica, M. E.; Epstein, A. J.; Tang, X. Synth Met 1992, 46, 337.
33. Inganas, O., Ed. Electroactive Polymers in Large Area Chromogenics; SPIE Institute Series 4; 1990; p 328.
34. Cao, Y.; Heeger, A. J. Synth Met 1990, 39, 205.
35. Larderich, T.; Tranayrd, P. Acad CR Sci Ser 1963, C84, 257.
36. Phol, H. A.; Engelhardt, E. H. J Phys Chem 1962, 66 2085.
37. Heeger, A. J Synth Met 1993, 55, 3471.
38. Yang, C. Y.; Reghu, M.; Heeger, A. J.; Cao, Y. Synth Met 1996, 79, 27.
39. Yang, S. M.; Li, C. P. Synth Met 1993, 55, 636.
40. Yang, S. M.; Chiang, J. H.; Shiah, W. M. Synth Met 1991, 41, 753.
41. Yang, S. M.; Shiah, W. M.; Lai, J. J. Synth Met 1991, 41, 757.
42. Yang, S. M.; Lin, T. S. Synth Met 1989, 29, E227.
43. Sun, L. F.; Liu, H. B.; Clark, R.; Yang, S. C. Synth Met 1997, 84, 67.
44. Liu, J. M.; Sun, L.; Yang, S. C. U.S. Pat. 5,489,400 (1996); p 6.
45. Liu, J. M.; Sun, L.; Hwang, J. H.; Yang, S. C. Mater Res Soc Symp Proc 1992, 247, 601.
46. Lin, D. S.; Yang, S. M. Synth Met 2001, 119, 111.
47. Vaivars, G.; Azens, A.; Granqvit, C. G. Solid State Ionics 1999, 119, 269.
48. McManus, P. M.; Cushman, R. J.; Yang, S. C. J Phys Chem 1987, 91, 744.
49. Cushman, R. J.; McManus, P. M.; Yang, S. C. J Electroanal Chem 1986, 291, 235.
50. Yang, S. M.; Chen, W. M.; You, K. S. Synth Met 1997, 84, 77.
51. Sun, L. F.; Yang, S. C.; Liu, T. M.; Abstr Paper Am Chem Soc 1992, 204, 137.
52. Weil, J. A.; Botton, J. R.; Wertz, J. E. Electron Spin Resonance: Elementary Theory and Practical Applications; Wiely-Interscience: New York, 1994.
53. Drago, R. S. Physical Method in Chemistry; Saunders College Publishing: Philadelphia, 1977.
54. Nechtschein, M.; Genoud, F. Solid State Commun 1994, 91, 471.
55. Aasmundtveit, K.; Genoud, F.; Houze, E.; Nechtschein, M. Synth Met 1995, 69, 193.
56. Lee, W.; Du, G.; Long, S. M.; Epstein, A. J.; Shimizu, S.; Saitoh, T.; Uzawa, M. Synth Met 1997, 84, 807.
57. Zhang, Q.; Jin, H.; Wang, X.; Jing, X. Synth Met 2001, 123, 481.
58. Andrei, M.; Roggero, A.; Marchese, L.; Passerini, S. Polymer 1994, 35, 3592.
59. Shizukuishi, M.; Inoue, E.; Kaga, E.; Kokado, H.; Shimizu, I. J Appl Phys 1981, 20, 581.
60. Morita, M. J Polym Sci Part B: Polym Phys 1994, 32, 231.
61. Denesuk, M.; Cronin, J. P.; Kennedy, S. R.; Uhlmann, D. R. J Electrochem Soc 1997, 144, 2154.
62. Yang, C. H.; Wen, T. C. J Electrochem Soc 1994, 141, 2624.